



HAL
open science

The diatom *Phaeodactylum tricornutum* adjusts NPQ capacity in response to dynamic light via fine-tuned Lhcx and xanthophyll cycle pigment synthesis

Bernard Lepetit, Gautier G lin, Mariana Lepetit, Sabine Sturm, Sascha Vugrinec, Alessandra Rogato, Peter G Kroth, Angela Falciatore, Johann Lavaud

► To cite this version:

Bernard Lepetit, Gautier G lin, Mariana Lepetit, Sabine Sturm, Sascha Vugrinec, et al.. The diatom *Phaeodactylum tricornutum* adjusts NPQ capacity in response to dynamic light via fine-tuned Lhcx and xanthophyll cycle pigment synthesis. *New Phytologist*, 2017, 214 (1), pp.205-218. <10.1111/nph.14337>. <hal-02324509>

HAL Id: hal-02324509

<https://hal.science/hal-02324509v1>

Submitted on 21 Oct 2019

HAL is a multi-disciplinary open access archive for the deposit and dissemination of scientific research documents, whether they are published or not. The documents may come from teaching and research institutions in France or abroad, or from public or private research centers.

L'archive ouverte pluridisciplinaire **HAL**, est destin e au d p t et   la diffusion de documents scientifiques de niveau recherche, publi s ou non,  manant des  tablissements d'enseignement et de recherche fran ais ou  trangers, des laboratoires publics ou priv s.



HAL Authorization

1 **The diatom *Phaeodactylum tricornutum* adjusts NPQ capacity in response to dynamic**
2 **light via fine-tuned Lhcx and xanthophyll cycle pigment synthesis**

3

4 Running title: NPQ capacity under dynamic light in *P. tricornutum*

5

6 Bernard Lepetit^{1,2*}, Gautier Gélín¹, Mariana Lepetit¹, Sabine Sturm², Sascha Vugrinec²,
7 Alessandra Rogato^{3,4}, Peter G. Kroth², Angela Falciatore⁵, Johann Lavaud^{1,6}

8 ¹ UMR7266 'LIENSs', CNRS Université de La Rochelle, Institut du littoral et de
9 l'Environnement, 2 rue Olympe de Gouges, 17000 La Rochelle, France

10 ² Zukunftskolleg, Pflanzliche Ökophysiologie, Universität Konstanz, 78457 Konstanz,
11 Germany

12 ³ Institute of Biosciences and BioResources, CNR, Via P. Castellino 111, 80131 Naples, Italy

13 ⁴ Stazione Zoologica Anton Dohrn Villa Comunale 80121 Naples, Italy

14 ⁵ Sorbonne Universités, UPMC, Institut de Biologie Paris-Seine, CNRS, Laboratoire de
15 Biologie Computationnelle et Quantitative, 15 rue de l'Ecole de Médecine, 75006 Paris,
16 France

17 ⁶ UMI 3376 TAKUVIK, CNRS/Université Laval, Département de Biologie, Pavillon
18 Alexandre-Vachon, 1045 avenue de la Médecine, Québec (Québec) G1V 0A6, Canada

19

20 *Corresponding author:

21 Bernard Lepetit
22 Zukunftskolleg, Pflanzliche Ökophysiologie, Universität Konstanz, 78457 Konstanz,
23 Germany

24 E-mail: Bernard.Lepetit@uni-konstanz.de

25 Phone: +49 7531 883133

26

27 Total word count main body: 6485

28 Introduction word count: 1152

29 Materials and Methods word count: 1392

30 Results word count: 1651

31 Discussion word count: 1888

32 Conclusion word count: 261

33 Acknowledgement word count: 141

34 10 Figures, 5 Figures and 1 Table in the Supporting Information

35 Summary

- 36 • Diatoms contain a highly flexible capacity to dissipate excessively absorbed light by
37 “Non-Photochemical fluorescence Quenching” (NPQ) based on the light induced
38 conversion of diadinoxanthin (Dd) into diatoxanthin (Dt) and the presence of Lhcx
39 proteins. Their NPQ fine regulation on the molecular level upon a shift to dynamic
40 light conditions is unknown.
- 41 • We investigated the regulation of Dd+Dt amount, Lhcx gene and protein synthesis and
42 NPQ capacity in the diatom *Phaeodactylum tricornutum* after a change from
43 continuous low light to three days of sine (SL) or fluctuating (FL) light conditions.
44 Four *P. tricornutum* strains with different NPQ capacities due to different expression
45 of *Lhcx1* were included.
- 46 • All strains responded to dynamic light comparably, independently of initial NPQ
47 capacity. During SL, NPQ capacity was strongly enhanced due to a gradual increase of
48 Lhcx2 and Dd+Dt amount. During FL, cells enhanced their NPQ capacity at the first
49 day due to increased Dd+Dt, Lhcx2 and Lhcx3; already at the second day light
50 acclimation was accomplished. While quenching efficiency of Dt was strongly
51 lowered during SL conditions, it remained high throughout the whole FL exposure.
- 52 • Our results highlight a more balanced and cost-effective photoacclimation strategy of
53 *P. tricornutum* under FL than under SL conditions.

54

55

56 Keywords: diatoms, dynamic light, Lhcx, NPQ, *Phaeodactylum tricornutum*, photoprotection,
57 xanthophyll cycle

58 **Introduction**

59 Diatoms are unicellular microalgae constituting one of the most important phytoplankton
60 groups in terms of biodiversity (Mann & Vanormelingen, 2013) and productivity (about 45 %
61 of marine carbon fixation) (Geider *et al.*, 2001). They strongly participate in the biological
62 carbon pump and the functioning of contemporary aquatic ecosystems (Armbrust, 2009). Due
63 to their high productivity and high lipid content, diatoms could potentially replace American
64 fossil oil consumption in the future (Levitani *et al.*, 2014) or be used for production of high
65 quality plastics (Roesle *et al.*, 2014). A peculiar feature of diatoms is their ability to live in
66 turbulent waters, where they can benefit from high nutrient availabilities (Tozzi *et al.*, 2004).
67 In such habitats light intensity changes over several orders of magnitude on the timescale of
68 minutes (Long *et al.*, 1994; MacIntyre *et al.*, 2000; Lavaud, 2007), therefore flexible
69 photosynthesis and efficient photoprotection mechanisms are necessary to avoid over-
70 excitation of the photosynthetic apparatus which would lead to the generation of reactive
71 oxygen species (ROS), eventually resulting in cell death (Niyogi & Truong, 2013). Diatoms
72 possess both, an unusual flexibility of photosynthetic productivity (Wilhelm *et al.*, 2006;
73 Kroth *et al.*, 2008; Lepetit *et al.*, 2012; Bailleul *et al.*, 2015), and effective photoprotection
74 mechanisms which include: 1) a fast operating PSII electron cycle (Lavaud *et al.*, 2002c;
75 Wagner *et al.*, 2016), 2) a tuneable amount of membrane dissolved xanthophylls
76 diadinoxanthin (Dd) and diatoxanthin (Dt) acting as antioxidants (Lepetit *et al.*, 2010), and 3)
77 a high capacity for dissipation of excess excitation energy, illustrated by non-photochemical
78 fluorescence quenching (NPQ) (Lavaud & Goss, 2014). NPQ in plants and green algae is
79 divided into three to four subtypes, which are not similarly well defined in diatoms (Lavaud &
80 Goss, 2014; Goss & Lepetit, 2015). Here we will refer to NPQ as a photoprotective
81 mechanism whose induction depends upon three regulatory components: (1) The proton
82 gradient generated between the thylakoid lumen and the chloroplast stroma during light
83 exposure (ΔpH), (2) a fast operating xanthophyll cycle (XC) through enzymatic conversion of
84 Dd into Dt in the presence of the ΔpH and the back conversion in its absence (i.e. typically in
85 the dark), and (3) chloroplast located, but nuclear encoded antenna proteins of the Light-
86 Harvesting Complex (LHC) superfamily. While Lhcf proteins build up the peripheral light
87 harvesting antenna (called “FCP”, likely predominantly associated with PSII *in vivo*)
88 (Grouneva *et al.*, 2011; Gundermann *et al.*, 2013; Nagao *et al.*, 2013; Schaller-Laudel *et al.*,
89 2015), Lhcr proteins form the PSI antenna (Veith *et al.*, 2009; Lepetit *et al.*, 2010; Grouneva
90 *et al.*, 2011; Ikeda *et al.*, 2013; Bina *et al.*, 2016). In contrast, Lhcx proteins are involved in
91 NPQ in the pennate diatom *Phaeodactylum tricornerutum* (Bailleul *et al.*, 2010; Lepetit *et al.*,

92 2013) and the centric *Thalassiosira pseudonana* (Zhu & Green, 2010; Wu *et al.*, 2012; Dong
93 *et al.*, 2015). Involvement of Lhcx proteins in photoprotection in other diatoms is also very
94 likely (Beer *et al.*, 2006; Park *et al.*, 2010; Laviale *et al.*, 2015; Ghazaryan *et al.*, 2016). It is
95 assumed that Lhcx proteins bind Dd and Dt (Beer *et al.*, 2006; Lepetit *et al.*, 2013) and they
96 apparently influence the supramolecular organisation of the antenna complexes (Ghazaryan *et al.*
97 *et al.*, 2016). The location of Lhcx within thylakoids remains ambiguous as based on contrasting
98 reports of both FCP (Beer *et al.*, 2006; Lepetit *et al.*, 2010; Grouneva *et al.*, 2011; Nagao *et al.*
99 *et al.*, 2013; Schaller-Laudel *et al.*, 2015) and PSI association (Grouneva *et al.*, 2011). The
100 current NPQ model proposes two major quenching sites in diatoms (Miloslavina *et al.*, 2009;
101 Chukhutsina *et al.*, 2014, Lavaud & Goss, 2014; Derks *et al.*, 2015; Goss & Lepetit, 2015):
102 Quenching site 1 is mechanistically independent of Dt (Chukhutsina *et al.*, 2014) and is
103 formed rapidly mainly by detached, oligomeric antenna complexes due to the build-up of the
104 ΔpH , while quenching site 2 is located close to the PSII reaction centres and is directly
105 dependent on Dt formation. Quenching site 1 also exists in *P. tricornutum* (Miloslavina *et al.*,
106 2009), but in this species NPQ always relies on Dt (Lavaud *et al.*, 2002a; Goss *et al.*, 2006),
107 except under special (i.e. artificial) conditions (Lavaud & Kroth, 2006; Eisenstadt *et al.*, 2008;
108 Lepetit *et al.*, 2013). This apparent contradiction could not been fully solved so far, but an
109 indirect influence of Dt also on formation of quenching site 1 has been postulated (Lavaud &
110 Goss, 2014; Goss & Lepetit, 2015).

111 In different diatoms, the NPQ capacity, in relation to the light environment of the respective
112 planktonic and benthic habitat, can be rather variable. Diatoms that cope with sudden light
113 exposures, e.g. coastal planktonic and immotile estuarine sediment-inhabiting diatoms, show
114 a higher NPQ capacity than diatoms living in more stable water bodies (e.g. semi-enclosed
115 bays, open ocean) and the motile and photophobic sediment-inhabiting forms (Lavaud *et al.*,
116 2007; Dimier *et al.*, 2009; Barnett *et al.*, 2015). The same holds true for diatom species
117 adapted to the seasonally successive polar habitats (Petrou *et al.*, 2011). *P. tricornutum* is
118 cosmopolitan, but prefers habitats where light climate is unstable and reaches punctual but
119 regular high intensities, such as coasts, estuaries, or rocky pools (De Martino *et al.*, 2007).
120 Different *P. tricornutum* ecotypes have different and variable NPQ capacities (Lavaud &
121 Lepetit, 2013) that largely depend on the amount of Lhcx1 (Bailleul *et al.*, 2010).
122 Additionally, there is growing evidence that two other light regulated isoforms, Lhcx2 and
123 Lhcx3, may also participate to NPQ under prolonged light stress (Lepetit *et al.*, 2013; Taddei
124 *et al.*, 2016).

125 For several diatom species the influence of near-natural light conditions on the photosynthetic
126 performance and on growth has been thoroughly investigated (Kromkamp & Limbeek, 1993;
127 Litchman, 2000; Fietz & Nicklisch, 2002; Wagner *et al.*, 2006; Jakob *et al.*, 2007; van de Poll
128 *et al.*, 2007; Kropuenske *et al.*, 2009; Su *et al.*, 2012; Jallet *et al.*, 2016). As *P. tricornutum* is
129 one of the best characterized diatoms on the molecular level, we investigated its
130 photophysiology during acclimation from stable low light to dynamic and potentially stressful
131 light conditions with respect to the interplay between Dd+Dt synthesis, LhcX expression and
132 NPQ capacity. Sine light (SL) conditions simulated the rise and decline of the sun during a
133 cloudless day in a stable water body. Fluctuating light conditions (FL) superimposed the
134 effect of vertical cell movement along the water column in an idealized manner with a mixing
135 from and to the aphotic zone via the surface within periods of 30 minutes. We also aimed at
136 investigating the influence of the initial photoprotection capacity on the adjustment of NPQ
137 capacity to dynamic light. Therefore, we used two *P. tricornutum* ecotypes with different
138 initial NPQ capacities (i.e. low and high natural NPQ phenotypes, see Bailleul *et al.*, 2010),
139 but also strains with silenced or overexpressed *LhcX1* protein. Our results contribute to the
140 better understanding of the molecular fine-tuning of NPQ capacity during acclimation to
141 dynamic light conditions in pennate diatoms.

142

143 **Materials and Methods**

144 *Cell culturing and light treatments*

145 Experiments were performed in four *Phaeodactylum tricornutum* strains with different NPQ
146 capacities: (1) *P. tricornutum* strain 1 (Pt1, CCAP 1055/1); (2) Pt1sil; Pt1 strain which
147 contains an antisense construct against the *LhcX1* gene, leading to reduced LhcX1 protein
148 synthesis (Bailleul *et al.*, 2010); (3) *P. tricornutum* strain 4 (Pt4, UTEX 646); (4) Pt4ov; Pt4
149 strain which overexpresses the *LhcX1* gene. The full length cDNA of the *LhcX1* gene (JGI ID:
150 27278) was cloned downstream of the *FcpA* (*Lhcfl*) promoter into the pPha-T1
151 transformation vector (Zaslavskaja *et al.*, 2000). Pt4 cells were biolistically transformed with
152 this construct according to Kroth (2007). Positive clones were selected on ZeocinTM
153 containing solid medium plates. *LhcX1* overexpressing clones were screened based on their
154 NPQ capacity and amongst several clones showing increased NPQ capacity the one with the
155 highest NPQ was selected for the present experiments (Pt4ov). This clone has an identical
156 photosynthetic yield as the wildtype under low light conditions (data not shown), but shows

157 strongly increased *Lhcx1* gene expression (Fig. S1). All four strains were grown in airlift
158 tubes (4 cm diameter) at 20°C in a 16 h day/8 h night rhythm with a light intensity of 50 μmol
159 $\text{photons m}^{-2} \text{s}^{-1}$ (onset at 8:00) defined as low light (LL). Light was provided by computer
160 controlled flora LED units (CLF Plant Climatics, Germany) with all LEDs (white, blue, red
161 and far red) switched on. Cells were cultured in sterile Provasoli's enriched F/2 seawater
162 medium. Chlorophyll a (Chl a) concentration was determined as described in Lepetit *et al.*
163 (2013). Cells in logarithmic phase were adjusted with fresh F/2 medium to a concentration of
164 $1.4 \mu\text{g Chl a mL}^{-1}$ at 18:00 each day for four consecutive days. The 5th day (day 0), sampling
165 started (see "Sampling" below). The following three days (day 1 to day 3) two different
166 dynamic light treatments were applied during the day phase, provided by the flora LED
167 system: 1) SL with a maximum light intensity of 500 $\mu\text{mol photons m}^{-2} \text{s}^{-1}$ reached at 16:00
168 ($18.3 \text{ mol photons m}^{-2}$ integrated daily light dose), 2) two different FL treatments with 32 light
169 intervals in total, where maximum intensity was either 500 (FL 500, $4.5 \text{ mol photons m}^{-2}$
170 integrated daily light dose) or 1000 $\mu\text{mol photons m}^{-2} \text{s}^{-1}$ (FL 1000, $8.9 \text{ mol photons m}^{-2}$
171 integrated daily light dose) (Fig. 1). Light intensities were measured with a spherical quantum
172 sensor (US-SQS/L, Walz, Germany) in the centre of the airlift tubes. Due to the relatively
173 large diameter of the airlift tubes and the relatively dense algal culture, light attenuation was
174 steep, which, together with the bubbling of the cultures, led to a continuous micro-fluctuation
175 superimposed on both SL and FL. The specific light intensities for all dynamic treatments are
176 idealized and were calculated based on the formulas of Kroon *et al.* (1992) and as described in
177 Wagner *et al.* (2006), assuming a dense algal culture during FL conditions with exponential
178 light attenuation in the water column. During the whole experiment (day 0 to day 3), Chl a
179 concentration was determined daily at 18:00 and cultures were diluted with fresh F/2 medium
180 to a concentration of $1.4 \mu\text{g Chl a mL}^{-1}$, in order to prevent nutrient limitation and self-
181 shading.

182 *Sampling*

183 Cells were harvested with a sterile syringe via a tube drawn in the airlift flask which was
184 sealed except for sampling. For pigment analyses, 500 μl of cells were filtered each day at
185 11:00, 14:00 and 17:00 on an Isopore Polycarbonate filter $1.2 \mu\text{m}$ (Millipore, USA) and
186 immediately frozen in liquid nitrogen. Cells exposed to FL were additionally harvested during
187 the light maxima directly before the three indicated time points. For gene expression and
188 protein analyses, 15 and 23 mL of cell suspension, respectively, were harvested each day at
189 14:00 and centrifuged for 4 min at 4°C and 4000 g. The precipitated cells were resolved in 1

190 mL ice cooled phosphate buffered saline and centrifuged at 14000 g for 1 min. The pellet was
191 frozen in liquid nitrogen and stored at -80 °C until further analysis.

192 *Fluorescence analyses*

193 Cells harvested each day at 11:00, 14:00 and 17:00 were acclimated to 30 $\mu\text{mol photons m}^{-2} \text{s}^{-1}$
194 for 30 min before measuring the maximum photosynthetic efficiency of PSII as $(F_m - F_o)/F_m$
195 $= F_v/F_m$ with an Aqua Pen (PSI Instruments, Czech Republic). In order to take into account
196 slower relaxing NPQ processes and to assess the maximum NPQ capacity, rapid light curves,
197 measured with a Water PAM and an Imaging PAM (Walz, Germany), were recorded after 45
198 min acclimation to 30 $\mu\text{mol photons m}^{-2} \text{s}^{-1}$, by applying thirteen steps of increasing light
199 intensity up to 1250 $\mu\text{mol m}^{-2} \text{s}^{-1}$ with a respective duration of 30 s at 455 nm. Before the
200 onset of the actinic light and during each rapid light curve, an 800 ms pulse of 4000 μmol
201 $\text{photons m}^{-2} \text{s}^{-1}$ was applied to determine the maximum fluorescence levels F_m and F_m' ,
202 respectively. Maximum relative electron transport rates ($rETR_{\text{max}}$) and other photosynthetic
203 and photoprotective parameters were obtained by fitting the obtained values according to
204 Eilers & Peeters (1988) and Serodio & Lavaud (2011). A description of these parameters can
205 be found in Table S1.

206 *Pigment, transcript and protein analyses*

207 Pigment extraction and HPLC analysis were performed as described in Lepetit *et al.* (2013).
208 The de-epoxidation state was calculated as $DES = Dt/(Dd+Dt)$.

209 RNA extraction, cDNA synthesis, qPCR and quantification followed the protocol in Lepetit *et*
210 *al.* (2013), except that *RPS* (ribosomal protein S1, JGI ID: 44451) was used as the reference
211 gene instead of *I8s* due to a more stable transcript amount under our dynamic light
212 conditions. The primer sequences for *Lhcx1*, *Lhcx2* and *Lhcx3* are listed in Lepetit *et al.*
213 (2013). For *RPS* we used 5'-AATTCCTCGAAGTCAACCAGG-3' and 5'-
214 GTGCAAGAGACCGGACATAC-3' as forward and reverse primer, respectively, and for
215 *Lhcf2* the forward and reverse primer were 5'-GCCGATATCCCCAATGGATTT-3' and 5'-
216 CTTGGTCGAAGGAGTCCCATC-3', respectively.

217 Protein extraction and Western blot analysis followed the protocol described in Coesel *et al.*
218 (2009), but using a 14% Lithiumdodecylsulfate PAGE for protein separation. Samples
219 corresponding to an amount of 1 μg Chl a were loaded on the gel. Anti-FCP6 (Westermann &
220 Rhiel, 2005) was kindly provided by Dr. Erhard Rhiel (University of Oldenburg, Germany).
221 This antibody detects all Lhcx isoforms in *P. tricornutum* (Laviale *et al.*, 2015; Taddei *et al.*,
222 2016), but based on its sequence it has the highest affinity for Lhcx3 and the lowest affinity

223 for Lhcx2. Anti-FCP6 was applied in a 1:5000 dilution overnight. Accurate loading and
224 blotting was verified by correct transfer of pre-stained protein markers (Roti-Mark
225 BICOLOR, Roth, Germany) on the PVDF membrane (Amersham Hybond-P, GE Healthcare,
226 USA), by staining gels with the Coomassie R-250 Pierce Imperial Protein stain (Thermo
227 Fisher Scientific, USA) and by incubating the blot membrane with Anti-PsbB (CP47,
228 Agrisera, Sweden). Anti-PsbB detection was only used as a proxy for correct loading and
229 blotting, as the amount of CP47 has a high turnover under light stress conditions (Wu *et al.*,
230 2011). Antibody signals were detected using the ECL Plus chemiluminescence system (GE
231 Healthcare, USA) followed by x-ray film exposure. In order to compare relative Lhcx protein
232 expression within the time-course of the experiments, protein samples of each *P. tricornutum*
233 strain of either the SL or the FL 1000 experiment were loaded on a single gel. Antibody signal
234 intensities were quantified using ImageJ (<http://imagej.nih.gov/ij/>). For each blot several films
235 with different exposure and development times were produced, in order to avoid the
236 saturation of the immunodetection signal for Lhcx1 (due to its high abundance) and Lhcx3
237 (due to its highest affinity to the anti-FCP6), while also obtaining a signal for the weakly
238 visible Lhcx2 protein (due to its lowest affinity to anti-FCP6). Relative quantification of
239 Lhcx1 and Lhcx3 referred on the corresponding signal at unstressed conditions (day 0). As
240 Lhcx2 could not be detected at day 0, relative quantification was performed based on
241 comparison of Lhcx2 to the Lhcx3 value at day 0. For each experimental point (SL and FL
242 1000), the mean of all strains was calculated, except that Pt4ov was omitted from the analysis
243 of Lhcx1 expression due to its artificial regulation by the overexpressing *Lhcf1* promoter (see
244 “*Cell culturing and light treatments*”).

245 *Statistics*

246 Significance with a P value ≤ 0.05 was determined with Student’s t-test calculated with
247 SigmaPlot, but for gene expression we used the Pairwise Fixed Reallocation Randomization
248 Test performed by REST according to Pfaffl *et al.* (2002).

249

250 **Results**

251 *NPQ capacity and photosynthetic parameters during SL and FL conditions*

252 Before exposing cells to dynamic light conditions, we analysed their NPQ capacity under
253 stable low light growth conditions. NPQ capacity was highest in the Lhcx1 overexpressing
254 strain Pt4ov with values between 4 and 5 (Fig. 2, day 0). Pt1 showed an NPQ capacity of ~

255 2.5, Pt1sil of ~ 2 and Pt4 of ~ 1.8 (Fig. 2). These different NPQ capacities were mainly due to
256 different expression of the *Lhcx1* gene (Fig. S1), as already shown in Bailleul *et al.* (2010).
257 The very high NPQ capacity of the Pt4ov strain was achieved by driving *Lhcx1* gene
258 expression by the *Lhcf1* promoter, resulting in a more than 10 fold higher *Lhcx1* transcript
259 level (Fig. S1).

260 The rationale of working with *P. tricornutum* strains showing naturally or genetically-
261 manipulated differential NPQ capacities was to investigate whether these differences would
262 influence their acclimation to dynamic light conditions. There was a strong continuous rise of
263 NPQ capacity during the SL treatment (except in Pt4ov, see below), while under FL
264 conditions NPQ increased at the first day similarly as under SL conditions, but then slowed
265 down (Fig. 2). Importantly, the high NPQ strains (Pt1 and Pt4ov) still exhibited the highest
266 NPQ at the end of both dynamic light treatments. Pt4 eventually reached a higher or similar
267 NPQ as Pt1sil under SL and FL conditions, respectively. The Pt4ov strain behaved somewhat
268 differently, as there was no increase of NPQ on day 1 under SL. This is most likely due to the
269 pronounced decrease of *Lhcx1* gene expression (Fig. S1), as its overexpressing *Lhcf1*
270 promoter is repressed under light stress (Nymark *et al.*, 2009). However, from day 2 on Pt4ov
271 also started to increase NPQ capacity. Interestingly, although under stable LL conditions (i.e.
272 day 0) Pt4ov had already higher NPQ values than the other strains at the end of FL treatment,
273 it further increased NPQ during FL exposure (Fig. 2). All these results did not indicate a
274 strong influence of initial NPQ capacity on the NPQ adjustment to dynamic light; instead, all
275 strains responded in a similar manner by increasing their NPQ capacity. As the standard errors
276 were rather high due to the dynamic nature of the experiment, in the following we combined
277 results of the different strains in order to better reveal the specific response of *P. tricornutum*
278 to the very distinct dynamic light conditions. This way, it became directly apparent that the
279 doubling of light intensity under FL 1000 conditions led to no further increase of NPQ
280 compared to FL 500 conditions. Actually, with a final value of ~ 3.2 the NPQ was almost
281 identical at both FL conditions, while it was 5.8 under SL conditions (Fig. 3).

282 The maximum photosynthetic yield of PSII gradually decreased during SL conditions,
283 especially during day 3, to 0.55 (20 % decrease), illustrating the appearance of
284 photoinhibition (Fig. 4a). In contrast, F_v/F_m was maintained high (~ 0.65) during FL
285 conditions. Again, no differences between FL 500 and FL 1000 conditions were observed
286 (data not shown, but can be seen from the minimal error bars in Fig. 4a). Because also no
287 major differences between FL 500 and FL 1000 conditions could be observed during the

288 follow-up experiments, data were combined (unless otherwise noted), in order to highlight
289 significant differences compared to SL.

290 Under SL conditions, $rETR_{max}$ (see Table S1 for the definition of the parameters) dropped
291 during the first day and slightly increased over the next two days compared to LL (Fig. 4b). In
292 contrast, $rETR_{max}$ did not change during the first day of FL, but strongly increased during day
293 2 and 3. α decreased by roughly 20 % already during the first day of SL and then stabilized
294 (Fig. 4c). It didn't remarkably change under FL conditions. Interestingly, there was no major
295 change in E_k between SL and FL conditions (Fig. 4d). It increased by ~ 50 % during day 2
296 and stabilized over day 3. The apparent low E_k values were likely due to the blue light of the
297 Imaging-PAM excitation beam and are in line with previous E_k values obtained the same way
298 (Serodio & Lavaud, 2011). Huge differences were observed in NPQ_{EK}/NPQ_{max} . It increased
299 from ~7 % in LL to almost 20 % under SL conditions, while under FL it even decreased (Fig.
300 4e). In line with this, also $E50_{NPQ}$ behaved differently: At first it decreased, but then increased
301 under both conditions. However, while the final $E50_{NPQ}$ value under SL conditions was
302 similar as under LL, it was more than 1.5 fold higher under FL conditions (Fig. 4f).

303 *Pigment stoichiometry during SL and FL*

304 The Chl a increase per day per culture volume (μ_{Chla}) strongly differed under both dynamic
305 conditions. Under SL conditions, μ_{Chla} dramatically decreased by 50 % on day 1 (compared to
306 LL) and by 80 % over the rest of the experiment (Fig. 5). In contrast, under FL conditions a
307 slight decrease of μ_{Chla} occurred during the first day, while already from the second day on the
308 cultures produced as much Chl a per day as during LL conditions. For both, the Chl c to Chl a
309 and the Fx to Chl a ratio, no remarkable differences between SL and FL conditions could be
310 observed (Fig. S2).

311 In general, changes of the NPQ capacity were well reflected by changes in the amount of XC
312 pigments. Dd+Dt increased 3.4 fold during SL treatment, reaching its maximum on the last
313 day (Fig. 6). Although most of the increase already occurred during day 1, the XC pool size
314 steadily increased during day 2 and 3 with repeated drops at night. In contrast, under FL
315 conditions the increase of XC pigments was only 1.7 fold, and the largest part of XC pigments
316 was also synthesized on day 1. The observed trend was identical in all strains under both light
317 conditions, although Pt1 strains synthesized more Dd+Dt than Pt4 strains (Fig. S3).

318 The DES ($Dt/(Dd+Dt)$) reached values of around 50 % during the first day of SL at 14:00 (6
319 hours after light onset) and 17:00 (9 hours after light onset) (Fig. S4). During the following

320 SL days and during all three days of FL conditions DES was lowest in the morning (11:00, 3
321 hours after light onset) and highest in the afternoon (17:00), in line with the respective light
322 intensities). During the light intervals of FL conditions, DES reached similar values as under
323 SL conditions, but always decreased below 10 % during the subsequent low light/dark phases,
324 indicating that Dt epoxidation took place rapidly during the decline of light intensity.

325 *NPQ versus Dd+Dt relationship*

326 The ratio of NPQ *versus* Dd+Dt is a robust indicator for the efficiency of the XC pigments to
327 confer NPQ (Lavaud & Lepetit, 2013; Lepetit *et al.*, 2013). NPQ/(Dd+Dt) strongly decreased
328 during the first day of SL treatment and recovered during the following days (Fig. 7). At the
329 last time point (day 3-17:00), it became statistically indistinguishable from day 0, indicating
330 that eventually Dt quenching efficiency reached the levels of LL acclimated cells. In contrast,
331 NPQ/(Dd+Dt) remained high under FL conditions, highlighting a high quenching efficiency
332 of Dt. During the second and third day it was statistically supported even higher at some time
333 points than under LL conditions.

334 *Lhcx gene expression and protein synthesis*

335 In agreement with previous analyses for low light to high light shifts (Nymark *et al.*, 2009;
336 Lepetit *et al.*, 2013), cells of all *P. tricornutum* strains strongly increased the transcript
337 amounts of *Lhcx2* and *Lhcx3* under both SL and FL conditions, while *Lhcx1* was only slightly
338 more transcribed (Fig. S1; note that *Lhcx1* transcription in Pt4ov reacted differentially due to
339 the regulation of the *Lhcx1* gene by the *Lhcf1* promoter). This became even more obvious,
340 when comparing the mean values of all strains (Fig. 8a-c). Intriguingly, there was a strong
341 difference in *Lhcx2* and *Lhcx3* transcript amounts depending on the light climate: Under SL
342 conditions, *Lhcx2* transcription was much more pronounced than under FL. In contrast, *Lhcx3*
343 transcript level was higher under FL conditions. Transcription of *Lhcx2* and *Lhcx3* increased
344 throughout SL treatment, while under FL conditions the maximum transcript level was
345 already reached on day 1 (but note the decrease of *Lhcx3* transcription on day 2 and 3). *Lhcf2*
346 is one of the major classical light harvesting antenna proteins of the FCP under low light
347 conditions (Lepetit *et al.*, 2010; Grouneva *et al.*, 2011; Gundermann *et al.*, 2013), hence under
348 stressful light conditions an expression pattern opposite to *Lhcx* genes was expected. Indeed,
349 there was a strong *Lhcf2* transcript reduction throughout the whole SL treatment (Fig. 8d). In
350 contrast, under FL conditions *Lhcf2* transcript levels dropped only during day 1, but reached
351 almost initial levels already by day 2.

352 In order to investigate whether the differences in *Lhcx* transcription between SL and FL
353 conditions were also reflected by the protein level, the Lhcx proteins were quantified. No
354 significant changes could be observed for Lhcx1 compared to LL conditions neither in SL nor
355 in FL (Fig. 9a). There was a gradual increase of Lhcx2 protein synthesis throughout the whole
356 SL experiment (Fig. 9b and Fig. S5 for an example of the Western blots obtained for Pt4),
357 while under FL conditions its level reached maximum values already on the second day and
358 was much lower compared to SL conditions on day 2 and day 3. In contrast, Lhcx3 content
359 similarly increased during day 1 under SL and FL, and declined during the following days
360 (Fig. 9c). Hence, only the Lhcx2 protein content correlated with the respective amounts of
361 transcripts, and both paralleled the increase in NPQ capacity under SL exposure (see Fig. 3).
362 This is better illustrated by plotting the mean relative amount of Lhcx2 versus the mean
363 increase of NPQ capacity under SL conditions of all strains (but Pt4ov due to its unusual NPQ
364 behaviour caused by the Lhcx1 overexpressing *Lhcf1* promoter), yielding a linear correlation
365 with an R^2 of 0.997 (Fig. 10).

366

367 **Discussion**

368 *Up-regulation of NPQ capacity is independent of initial NPQ capacity during acclimation to*
369 *dynamic light conditions*

370 We could not observe major differences in adjustment of NPQ capacity during dynamic light
371 conditions in the low NPQ strains (Pt1sil and Pt4) compared to the high NPQ strains (Pt1 and
372 Pt4ov). In line with this result, there was also no correlation between initial NPQ capacity and
373 XC pigment synthesis, the latter being strain dependent: Pt1 and Pt1sil showed a stronger
374 increase of Dd+Dt pool size than Pt4ov and Pt4 (Fig. S3). Furthermore, the Pt4ov strain,
375 which under LL already possessed an NPQ capacity as high as Pt1sil at the end of the SL
376 treatment (Fig. 2), similarly increased *Lhcx2* and *Lhcx3* gene expression as well as the Dd+Dt
377 pool size (Fig. S1 and Fig. S3). The apparently low influence of the initial NPQ capacity on
378 the subsequent NPQ adjustment during dynamic light conditions may be due to the fact that
379 initial NPQ capacity under stable LL conditions is first determined by Lhcx1 and Dd+Dt
380 amount (Bailleul *et al.*, 2010). As reported here for dynamic light and before for prolonged
381 high light conditions (Lepetit *et al.*, 2013), a higher NPQ capacity is obtained by the
382 combined increase of Dd+Dt pool size and primarily Lhcx2 expression.

383 Insights into the regulation of NPQ actors in diatoms have been gained recently, and clearly
384 photoreceptor mediated processes influence NPQ capacity (Schellenberger Costa *et al.*, 2013;

385 Brunet *et al.*, 2014). In line with this, the *Lhcx1* gene promoter has a binding motif for a blue
386 light receptor, aureochrome 1a (Schellenberger Costa *et al.*, 2013). The cryptochromes CPF
387 (Coesel *et al.*, 2009) and CryP (Juhás *et al.*, 2014) regulate expression of *Lhcx* genes.
388 Interestingly, in *Chlamydomonas reinhardtii* the cryptochrome aCRY, which is related to
389 CryP, seems to react rather on light intensity than on light quality (Beel *et al.*, 2012), hence
390 CryP could modulate NPQ capacity in diatoms in response to different light intensities.
391 Besides the influence of photoreceptors on NPQ adjustment, we previously demonstrated that
392 Dd+Dt increase and *Lhcx2* expression rates are controlled by changes in the redox state of the
393 PQ-pool, while *Lhcx3* expression may be regulated via ROS (Lepetit *et al.*, 2013; Lepetit &
394 Dietzel, 2015). In the present study *Lhcx2* expression and Dd+Dt content correlated well
395 under both dynamic light conditions, indicating the presence of a common trigger. Clearly,
396 the expression of *Lhcx2* and *Lhcx3* differed under SL and FL, suggesting that both light
397 conditions elicit two different regulation pathways, which is likely due to the different
398 characteristics of SL and FL in combination with their different total light doses. The PQ-pool
399 redox state responsive *Lhcx2* and Dd+Dt reacted rather gradually to long lasting light stimuli
400 under SL, which generated a higher cumulative photon amount per day. In contrast, *Lhcx3*
401 expression was regulated by short but intense light intervals, conditions which are expected to
402 generate pronounced amounts of ROS. Because the NPQ capacity has an influence on energy
403 flow into the electron transport chain and thus on the redox state of the PQ-pool and on ROS
404 generation (Triantaphylidès *et al.*, 2008; Kruk & Szymańska, 2012), the concentration of the
405 reduced PQ-pool and ROS should be different in the four *P. tricornutum* strains under
406 dynamic light conditions. Still, the four strains adjusted their NPQ capacity in a similar way
407 under dynamic light conditions. The fact that NPQ capacity increases even in the highest NPQ
408 strain (Pt4ov) illustrates that initial NPQ capacity was not sufficient to avoid partial over-
409 reduction of the electron transport chain. Sensitive PQ-pool redox state and ROS responding
410 promoter elements may already react to a partly reduced PQ-pool and small amounts of ROS,
411 so that minor differences in these triggers would hardly differentially affect the expression of
412 *Lhcx* genes and the synthesis of Dd+Dt pigments. Moreover, the redox state of the PQ-pool
413 can be influenced by changes of the metabolome (Jungandreas *et al.*, 2014; Wilhelm *et al.*,
414 2014; Levitan *et al.*, 2015). Such influences would be fairly independent of the NPQ capacity
415 and could also explain the similar NPQ response in the four *P. tricornutum* strains.

416

417 *Lhcx2* in combination with the amount of XC pigments likely increases NPQ capacity under
418 dynamic light

419 In diatoms, the increase of XC pigments does not necessarily lead to a higher NPQ
420 (Schumann *et al.*, 2007). Specific proteins must be synthesized to bind these pigments for an
421 effective involvement in NPQ (Lepetit *et al.*, 2013). *Lhcx1* does not increase significantly
422 during dynamic light conditions (Fig. 9a), and hence confers only basal NPQ capacity. In
423 *Lhcx2* or *Lhcx3* overexpression lines, both proteins provide additional NPQ capacity (Taddei
424 *et al.*, 2016). *Lhcx2* content similarly increased on day 1 in SL and FL conditions, and
425 remained stable during the following days in FL, while it increased in SL. These features were
426 paralleled by the NPQ capacity. In fact, *Lhcx2* amount was linearly correlated to the NPQ
427 capacity increase under SL conditions (Fig. 10). Although this correlation is based only on a
428 few data points, it suggests *Lhcx2* being a major actor in modelling NPQ capacity under
429 dynamic light conditions, together with the size of the XC pigment pool and the degree of de-
430 epoxidation.

431 The impact of *Lhcx3* on NPQ capacity enhancement is difficult to deduce. Our data suggest
432 that *Lhcx3* was less responsible for NPQ increase during day 2 and 3 in SL and FL, as its
433 protein content was rather decreasing (Fig. 9c). Instead, the prompt increase of *Lhcx3* on day
434 1 under both dynamic conditions may provide a fast increase of photoprotection capacity,
435 while *Lhcx2* continues to add up during prolonged light stress conditions like under SL
436 treatment. Interestingly, there was a significant difference in *Lhcx3* transcript levels between
437 FL and SL on day 1, which was not reflected by the protein level. This suggests that
438 posttranscriptional control mechanisms, that specifically respond to fast light intensity
439 fluctuations, partially prevent *Lhcx3* protein synthesis. In line with this, it was recently shown
440 in *A. thaliana* that high light regulation of several high light responsive target proteins often
441 occurs differentially on the transcriptional and translational level (Oelze *et al.*, 2014). An
442 additional control point at the *Lhcx3* translational level might be a strategy to acclimate the
443 NPQ system to an average light intensity delivered by light fluctuations, while keeping a high
444 *Lhcx3* transcript reservoir in case of prolonged light stress. This would avoid a too strong
445 down-regulation of photochemistry during low light periods, while ensuring sufficient excess
446 energy dissipation during high light regular peak exposures, a feature in line with the fast
447 on/off switch of the NPQ system (Lavaud *et al.*, 2007) and the fine regulation of Dd+Dt
448 synthesis versus the velocity of light fluctuations (Giovagnetti *et al.*, 2014) in diatoms.

449 Besides *Lhcx2*, and to some extent *Lhcx3*, other proteins could contribute to additional NPQ
450 capacity under dynamic light, especially to the slight increase of NPQ during FL on day 2 and

451 day 3. The *Lhcr* gene family contains a phylogenetically separated subclade (Nymark *et al.*,
452 2013), which genes are transcriptionally up-regulated during high light stress (Nymark *et al.*,
453 2009). The corresponding proteins may be at least partially involved in modulating NPQ
454 capacity. Another possible candidate is *Lhcf15*, which is the only *Lhcf* gene showing up-
455 regulation during short term light stress (Nymark *et al.*, 2009), but which especially responds
456 to red light (Schellenberger Costa *et al.*, 2013; Valle *et al.*, 2014; Herbstová *et al.*, 2015).
457 *Lhcf15* can build up specific antennae complexes with a red-shifted fluorescence emission
458 (Herbstová *et al.*, 2015), that could be correlated to the NPQ capacity (Lavaud & Lepetit,
459 2013).

460 *FL triggers a very effective photoprotective response*

461 Under SL conditions, the cells first synthesized much more Dd+Dt than could be used for
462 NPQ. Eventually, the ratio NPQ/(Dd+Dt) was better adjusted towards a higher quenching
463 efficiency of Dt due to a slowdown of Dd+Dt synthesis and a concomitant catch-up of *Lhcx2*
464 synthesis. Despite a strongly increased NPQ capacity as well as a massive reduction of Chl a
465 synthesis and *Lhcf2* transcription, decrease in photosynthetic efficiency could not be
466 completely prevented. In contrast, cells under FL conditions kept the NPQ/(Dd+Dt) efficiency
467 rather comparable to that of LL conditions, i.e. they synthesized only as many Dd+Dt as
468 actually could be used for providing an optimal effective involvement of Dt in NPQ. Parallel
469 to enhancing NPQ capacity, FL cells adjusted the reactivity of NPQ activation. The light
470 intensity, for which 50 % of the maximum NPQ capacity was reached, was shifted to much
471 higher values (Fig. 4f). Simultaneously, despite increasing E_k , FL cells kept the level of NPQ
472 activation at E_k very low (i.e. a few % of NPQ_{max} , Fig. 4e). This is noteworthy, because
473 although E_k increased similarly, SL cells were unable to adjust the threshold for NPQ onset
474 and activated a pronounced NPQ already at E_k . Ultimately, FL cells strongly increased
475 $rETR_{max}$, but kept α high as in LL cells, in line with previous results in *Skeletonema costatum*
476 (Kromkamp & Limbeek, 1993). All these changes enabled FL cells to use absorbed light
477 efficiently until E_k was reached and even beyond due to the moderate switch-on of NPQ.
478 Hence, they exploited as much light as possible for photochemistry during the short light
479 periods thanks to the adjustment of NPQ capacity and kinetics. Consequently, after one day of
480 acclimation, μ_{Chla} and *Lhcf2* transcription reached similar values as under LL conditions. As
481 FL cells developed a much higher NPQ capacity than LL cells, altogether FL acclimation
482 does not correspond to either a low or high light type strategy, but shows peculiar

483 characteristics. Such special fluctuating light acclimation strategy has also been observed in
484 the diatom *Stephanodiscus neoastraea* (Fietz & Nicklisch, 2002).

485 We have to note that the fine-acclimation to FL conditions with different intensity maximums
486 may be limited. Although FL 1000 cells faced much higher light intensities, steeper light
487 gradients and the double daily photon dose, NPQ capacity increased similarly as in FL 500
488 cells. On the one hand, this very similar NPQ pattern may be co-initiated by an internal
489 trigger such as the circadian clock. The influence of the circadian clock on the regulation of
490 the XC pigments in *P. tricornutum* has already been demonstrated (Ragni & d'Alcalà, 2007).
491 On the other hand, Giovagnetti *et al.* (2014) showed that light acclimation response in
492 *Pseudonitzschia multistriata* is triggered by light intensity, but also by the velocity of the light
493 increase. Moreover, in *Skeletonema marinoi*, NPQ capacity is not directly correlated to the
494 total daily photon dose (Orefice *et al.*, 2016). Our results suggest that, below a certain
495 duration threshold of regular light periods, different high light intensities only trigger an
496 efficient on/off reaction of NPQ capacity adjustment, but no fine-tuned response. This is
497 possibly due to the lack of the gradual PQ-pool signal. Interestingly, when the light intervals
498 become even shorter than the dark intervals in a fluctuating light regime, *P. tricornutum* is
499 able to generate a very high NPQ (Lavaud *et al.*, 2002b; Ruban *et al.*, 2004), which may not
500 be triggered by light, but may be elicited by darkness instead. As only the transcription of the
501 *Lhcx4* isoform is stimulated in the dark (Lepetit *et al.*, 2013; Nymark *et al.*, 2013) and the
502 respective protein can induce NPQ (Taddei *et al.*, 2016), *Lhcx4*, together with the increased
503 Dd+Dt content (Lavaud *et al.*, 2002b), may be responsible for this particular increased NPQ
504 capacity.

505 **Conclusion**

506 Our study highlights the importance of investigating the influence of dynamic light conditions
507 on NPQ in diatoms. Recently, it was shown that *P. tricornutum* is coping well with
508 fluctuating light conditions by possessing a low-cost PSII repair cycle compared to diatoms
509 living in the open ocean in more stable light conditions (Lavaud *et al.*, 2016). A
510 comprehensive study by Wagner *et al.* (2006) demonstrated that in *P. tricornutum* absorbed
511 photons are converted to a much higher extent into biomass in FL than in SL conditions,
512 which is due to a strongly decreased amount of alternative electrons and a lowered quantum
513 requirement per molecule oxygen evolved. The finely adjusted regulation of NPQ capacity by
514 balanced *Lhcx2/Lhcx3* and Dd+Dt synthesis under FL has three consequences which support
515 the observations of Wagner *et al.* (2006): (1) Investment costs for photoprotection

516 mechanisms are lower than in SL; (2) Photodamage is reduced, keeping costs for repair
517 processes low; (3) Too much photoprotection, leading to a poor light energy to chemical
518 energy conversion rate and hence to a high quantum requirement for carbon fixation, is
519 prevented. This latter feature has been recently demonstrated to be of global importance in the
520 upper ocean (Lin *et al.*, 2016). The better balanced photoacclimation strategy under FL
521 compared to SL conditions may be one reason why diatoms dominate in habitats where the
522 light climate is regularly punctuated with high intensity exposure periods, such as coastal
523 waters and estuarine intertidal sediments (Strzepek & Harrison, 2004; Lavaud *et al.*, 2007;
524 Dimier *et al.*, 2009; Petrou *et al.*, 2011; Barnett *et al.*, 2015).

525 **Acknowledgement**

526 We thank Dr. Torsten Jakob (Leipzig) for help with installing the dynamic light conditions,
527 Doris Ballert (Konstanz) for performing the biolistic transformation of the Pt4ov strain, Dr.
528 Erhard Rhiel (Oldenburg) for providing the FCP6 antibody and Dr. Giovanni Finazzi
529 (Grenoble) for valuable scientific discussion. We also thank the three reviewers for their
530 constructive criticism. This work was supported by the German Academic Exchange Service-
531 DAAD (postdoctoral grant to B.L.), an Marie Curie Zukunftskolleg Incoming Fellowship,
532 University of Konstanz (grant no. 291784, to B.L.), a University of Konstanz Zukunftskolleg
533 Interim grant (to B.L.), the Centre National de la Recherche Scientifique and the French
534 consortium Contrat de Plan État-Région Littoral (grants to J.L.), the Deutsche
535 Forschungsgemeinschaft (grant nos. LE 3358/3-1 to B.L., LA-2368/2-1 to J.L., and KR-
536 1661/7-1 to P.G.K.), and the Marie-Curie ITN CALIPSO (ITN 2013 GA 607607, to A.F.).

537

538 **Author contribution**

539 B.L., P.G.K., A.F. and J.L. designed research. B.L., G.G., M.L., S.S., S.V., A.R. and J.L.
540 performed experiments. B.L. and J.L. analysed data. B.L., A.F. and J.L. interpreted results.
541 B.L., A.R., P.G.K., A.F. and J.L. wrote the manuscript.

542

543

544 **Reference list**

545 **Armbrust EV. 2009.** The life of diatoms in the world's oceans. *Nature* **459**: 185-192.

546
547 **Bailleul B, Berne N, Murik O, Petroustos D, Prihoda J, Tanaka A, Villanova V, Bligny**
548 **R, Flori S, Falconet D et al. 2015.** Energetic coupling between plastids and mitochondria
549 drives CO₂ assimilation in diatoms. *Nature* **524**: 366-369.

550
551 **Bailleul B, Rogato A, de Martino A, Coesel S, Cardol P, Bowler C, Falciatore A, Finazzi**
552 **G. 2010.** An atypical member of the light-harvesting complex stress-related protein family
553 modulates diatom responses to light. *Proceedings of the National Academy of Sciences of the*
554 *United States of America* **107**: 18214-18219.

555
556 **Barnett A, Méléder V, Blommaert L, Lepetit B, Gaudin P, Vyverman W, Sabbe K,**
557 **Dupuy C, Lavaud J. 2015.** Growth form defines physiological photoprotective capacity in
558 intertidal benthic diatoms. *The ISME journal* **9**: 32-45.

559
560 **Beel B, Prager K, Spexard M, Sasso S, Weiss D, Müller N, Heinnickel M, Dewez D,**
561 **Ikoma D, Grossman AR et al. 2012.** A flavin binding cryptochrome photoreceptor responds
562 to both blue and red light in *Chlamydomonas reinhardtii*. *The Plant Cell* **24**: 2992-3008.

563
564 **Beer A, Gundermann K, Beckmann J, Büchel C. 2006.** Subunit composition and
565 pigmentation of fucoxanthin-chlorophyll proteins in diatoms: Evidence for a subunit involved
566 in diadinoxanthin and diatoxanthin binding. *Biochemistry* **45**: 13046-13053.

567
568 **Bína D, Herbstová M, Gardian Z, Vácha F, Litvín R. 2016.** Novel structural aspect of the
569 diatom thylakoid membrane: lateral segregation of photosystem I under red-enhanced
570 illumination. *Scientific reports* **6**: 25583.

571
572 **Brunet C, Chandrasekaran R, Barra L, Giovagnetti V, Corato F, Ruban AV. 2014.**
573 Spectral radiation dependent photoprotective mechanism in the diatom *Pseudo-nitzschia*
574 *multistriata*. *PLoS One* **9**: e87015.

575
576 **Chukhutsina VU, Büchel C, van Amerongen H. 2014.** Disentangling two non-
577 photochemical quenching processes in *Cyclotella meneghiniana* by spectrally-resolved
578 picosecond fluorescence at 77K. *Biochimica et Biophysica Acta (BBA)-Bioenergetics* **1837**:
579 899-907.

580
581 **Coesel S, Mangogna M, Ishikawa T, Heijde M, Rogato A, Finazzi G, Todo T, Bowler C,**
582 **Falciatore A. 2009.** Diatom PtCPF1 is a new cryptochrome/photolyase family member with
583 DNA repair and transcription regulation activity. *Embo Reports* **10**: 655-661.

584

585 **De Martino A, Meichenin A, Shi J, Pan K, Bowler C. 2007.** Genetic and phenotypic
586 characterization of *Phaeodactylum tricornutum* (Bacillariophyceae) accessions. *Journal of*
587 *Phycology* **43**: 992-1009.

588
589 **Derks A, Schaven K, Bruce D. 2015.** Diverse mechanisms for photoprotection in
590 photosynthesis. Dynamic regulation of photosystem II excitation in response to rapid
591 environmental change. *Biochimica et Biophysica Acta (BBA)-Bioenergetics* **1847**: 468-485.

592
593 **Dimier C, Giovanni S, Ferdinando T, Brunet C. 2009.** Comparative ecophysiology of the
594 xanthophyll cycle in six marine phytoplanktonic species. *Protist* **160**: 397-411.

595
596 **Dong Y-L, Jiang T, Xia W, Dong H-P, Lu S-H, Cui L. 2015.** Light harvesting proteins
597 regulate non-photochemical fluorescence quenching in the marine diatom *Thalassiosira*
598 *pseudonana*. *Algal Research* **12**: 300-307.

599
600 **Eilers P, Peeters J. 1988.** A model for the relationship between light intensity and the rate of
601 photosynthesis in phytoplankton. *Ecological modelling* **42**: 199-215.

602
603 **Eisenstadt D, Ohad I, Keren N, Kaplan A. 2008.** Changes in the photosynthetic reaction
604 centre II in the diatom *Phaeodactylum tricornutum* result in non-photochemical fluorescence
605 quenching. *Environmental Microbiology* **10**: 1997-2007.

606
607 **Fietz S, Nicklisch A. 2002.** Acclimation of the diatom *Stephanodiscus neoastraea* and the
608 cyanobacterium *Planktothrix agardhii* to simulated natural light fluctuations. *Photosynthesis*
609 *Research* **72**: 95-106.

610
611 **Geider RJ, Delucia EH, Falkowski PG, Finzi AC, Grime JP, Grace J, Kana TM, La**
612 **Roche J, Long SP, Osborne BA et al. 2001.** Primary productivity of planet earth: biological
613 determinants and physical constraints in terrestrial and aquatic habitats. *Global Change*
614 *Biology* **7**: 849-882.

615
616 **Ghazaryan A, Akhtar P, Garab G, Lambrev PH, Büchel C. 2016.** Involvement of the
617 Lhcx protein Fcp6 of the diatom *Cyclotella meneghiniana* in the macro-organisation and
618 structural flexibility of thylakoid membranes. *Biochimica et Biophysica Acta (BBA)-*
619 *Bioenergetics* **1857**: 1373-1379.

620
621 **Giovagnetti V, Flori S, Tramontano F, Lavaud J, Brunet C. 2014.** The velocity of light
622 intensity increase modulates the photoprotective response in coastal diatoms. *PLoS One* **9**:
623 e103782.

624
625 **Goss R, Lepetit B. 2015.** Biodiversity of NPQ. *Journal of Plant Physiology* **172**: 13-32.

626

627 **Goss R, Pinto EA, Wilhelm C, Richter M. 2006.** The importance of a highly active and
628 delta pH regulated diatoxanthin epoxidase for the regulation of the PSII antenna function in
629 diadinoxanthin cycle containing algae. *Journal of Plant Physiology* **163**: 1008-1021.

630

631 **Grouneva I, Rokka A, Aro EM. 2011.** The thylakoid membrane proteome of two marine
632 diatoms outlines both diatom-specific and species-specific features of the photosynthetic
633 machinery. *Journal of Proteome Research* **10**: 5338-5353.

634

635 **Gundermann K, Schmidt M, Weisheit W, Mittag M, Büchel C. 2013.** Identification of
636 several sub-populations in the pool of light harvesting proteins in the pennate diatom
637 *Phaeodactylum tricorutum*. *Biochimica et Biophysica Acta (BBA) - Bioenergetics* **1827**: 303-
638 310.

639

640 **Herbstová M, Bína D, Koník P, Gardian Z, Vácha F, Litvín R. 2015.** Molecular basis of
641 chromatic adaptation in pennate diatom *Phaeodactylum tricorutum*. *Biochimica et*
642 *Biophysica Acta (BBA) - Bioenergetics* **1847**: 534-543.

643

644 **Ikeda Y, Yamagishi A, Komura M, Suzuki T, Dohmae N, Shibata Y, Itoh S, Koike H,**
645 **Satoh K. 2013.** Two types of fucoxanthin-chlorophyll-binding proteins I tightly bound to the
646 photosystem I core complex in marine centric diatoms. *Biochimica et Biophysica Acta (BBA)-*
647 *Bioenergetics* **1827**: 529-539.

648

649 **Jakob T, Wagner H, Stehfest K, Wilhelm C. 2007.** A complete energy balance from
650 photons to new biomass reveals a light- and nutrient-dependent variability in the metabolic
651 costs of carbon assimilation. *Journal of Experimental Botany* **58**: 2101-2112.

652

653 **Jallet D, Caballero MA, Gallina AA, Youngblood M, Peers G. 2016.** Photosynthetic
654 physiology and biomass partitioning in the model diatom *Phaeodactylum tricorutum* grown
655 in a sinusoidal light regime. *Algal Research* **18**: 51-60.

656

657 **Juhas M, Zadow A, Spexard M, Schmidt M, Kottke T, Büchel C. 2014.** A novel
658 cryptochrome in the diatom *Phaeodactylum tricorutum* influences the regulation of light
659 harvesting protein levels. *Febs Journal* **281**: 2299-2311.

660

661 **Jungandreas A, Costa BS, Jakob T, von Bergen M, Baumann S, Wilhelm C. 2014.** The
662 acclimation of *Phaeodactylum tricorutum* to blue and red light does not influence the
663 photosynthetic light reaction but strongly disturbs the carbon allocation pattern. *PLoS One* **9**:
664 e99727.

665

666 **Kromkamp J, Limbeek M. 1993.** Effect of short-term variation in irradiance on light
667 harvesting and photosynthesis of the marine diatom *Skeletonema costatum*: a laboratory study
668 simulating vertical mixing. *Journal of general microbiology* **139**: 2277-2284.

669

670 **Kroon BMA, Hes UM, Mur LR. 1992.** An algal cyclostat with computer-controlled
671 dynamic light regime. *Hydrobiologia* **238**: 63-70.

672

673 **Kropuenske LR, Mills MM, van Dijken GL, Bailey S, Robinson DH, Welschmeyer NA,**
674 **Arrigoa KR. 2009.** Photophysiology in two major Southern Ocean phytoplankton taxa:
675 photoprotection in *Phaeocystis antarctica* and *Fragilariopsis cylindrus*. *Limnology and*
676 *Oceanography* **54**: 1176-1196.

677

678 **Kroth PG. 2007.** Genetic transformation - a tool to study protein targeting in diatoms. In:
679 Van der Giezen M, ed. *Methods in Molecular Biology - Protein Targeting Protocols*. Totowa
680 (New Jersey), USA: Humana Press, 257-268.

681

682 **Kroth PG, Chiovitti A, Gruber A, Martin-Jezequel V, Mock T, Parker MS, Stanley MS,**
683 **Kaplan A, Caron L, Weber T et al. 2008.** A model for carbohydrate metabolism in the
684 diatom *Phaeodactylum tricornutum* deduced from comparative whole genome analysis. *PLoS*
685 *One* **3**: e1426.

686

687 **Kruk J, Szymańska R. 2012.** Singlet oxygen and non-photochemical quenching contribute
688 to oxidation of the plastoquinone-pool under high light stress in Arabidopsis. *Biochimica et*
689 *Biophysica Acta (BBA)-Bioenergetics* **1817**: 705-710.

690

691 **Lavaud J. 2007.** Fast regulation of photosynthesis in diatoms: mechanisms, evolution and
692 ecophysiology. *Functional Plant Science and Biotechnology* **1**: 267-287.

693

694 **Lavaud J, Goss R. 2014.** The peculiar features of non-photochemical fluorescence quenching
695 in diatoms and brown algae. In: Demmig-Adams B, Garab G, Adams III W, Govindjee, eds.
696 *Non-Photochemical Quenching and Energy Dissipation in Plants, Algae and Cyanobacteria*.
697 Dordrecht, The Netherlands: Springer, 421-443.

698

699 **Lavaud J, Kroth PG. 2006.** In diatoms, the transthylakoid proton gradient regulates the
700 photoprotective non-photochemical fluorescence quenching beyond its control on the
701 xanthophyll cycle. *Plant and Cell Physiology* **47**: 1010-1016.

702

703 **Lavaud J, Lepetit B. 2013.** An explanation for the inter-species variability of the
704 photoprotective non-photochemical chlorophyll fluorescence quenching in diatoms.
705 *Biochimica et Biophysica Acta (BBA) - Bioenergetics* **1827**: 294-302.

706

707 **Lavaud J, Rousseau B, Etienne AL. 2002a.** In diatoms, a transthylakoid proton gradient
708 alone is not sufficient to induce a non-photochemical fluorescence quenching. *FEBS Letters*
709 **523**: 163-166.

710

711 **Lavaud J, Rousseau B, Van Gorkom HJ, Etienne AL. 2002b.** Influence of the
712 diadinoxanthin pool size on photoprotection in the marine planktonic diatom *Phaeodactylum*
713 *tricornutum*. *Plant Physiology* **129**: 1398-1406.

714
715 **Lavaud J, Six C, Campbell DA. 2016.** Photosystem II repair in marine diatoms with
716 contrasting photophysiology. *Photosynthesis Research* **127**: 189-199.

717
718 **Lavaud J, Strzepek RF, Kroth PG. 2007.** Photoprotection capacity differs among diatoms:
719 Possible consequences on the spatial distribution of diatoms related to fluctuations in the
720 underwater light climate. *Limnology and Oceanography* **52**: 1188-1194.

721
722 **Lavaud J, Van Gorkom HJ, Etienne AL. 2002c.** Photosystem II electron transfer cycle and
723 chlororespiration in planktonic diatoms. *Photosynthesis Research* **74**: 51-59.

724
725 **Laviale M, Barnett A, Ezequiel J, Lepetit B, Frankenbach S, Méléder V, Serôdio J,**
726 **Lavaud J. 2015.** Response of intertidal benthic microalgal biofilms to a coupled light-
727 temperature stress: evidence for latitudinal adaptation along the Atlantic coast of Southern
728 Europe. *Environmental Microbiology* **117**: 3662-3677.

729
730 **Lepetit B, Dietzel L. 2015.** Light signaling in photosynthetic eukaryotes with ‘green’ and
731 ‘red’ chloroplasts. *Environmental and Experimental Botany* **114**: 30-47.

732
733 **Lepetit B, Goss R, Jakob T, Wilhelm C. 2012.** Molecular dynamics of the diatom thylakoid
734 membrane under different light conditions. *Photosynthesis Research* **111**: 245-257.

735
736 **Lepetit B, Sturm S, Rogato A, Gruber A, Sachse M, Falciatore A, Kroth PG, Lavaud J.**
737 **2013.** High light acclimation in the secondary plastids containing diatom *Phaeodactylum*
738 *tricornutum* is triggered by the redox state of the plastoquinone pool. *Plant Physiology* **161**:
739 853-865.

740
741 **Lepetit B, Volke D, Gilbert M, Wilhelm C, Goss R. 2010.** Evidence for the existence of one
742 antenna-associated, lipid-dissolved, and two protein-bound pools of diadinoxanthin cycle
743 pigments in diatoms. *Plant Physiology* **154**: 1905-1920.

744
745 **Levitan O, Dinamarca J, Hochman G, Falkowski PG. 2014.** Diatoms: a fossil fuel of the
746 future. *Trends in biotechnology* **32**: 117-124.

747
748 **Levitan O, Dinamarca J, Zelzion E, Gorbunov MY, Falkowski PG. 2015.** An RNA
749 interference knock-down of nitrate reductase enhances lipid biosynthesis in the diatom
750 *Phaeodactylum tricornutum*. *The Plant Journal* **84**: 963-973.

751
752 **Lin H, Kuzminov FI, Park J, Lee S, Falkowski PG, Gorbunov MY. 2016.** Phytoplankton.
753 The fate of photons absorbed by phytoplankton in the global ocean. *Science* **351**: 264-267.

754
755 **Litchman E. 2000.** Growth rates of phytoplankton under fluctuating light. *Freshwater*
756 *Biology* **44**: 223-235.

757
758 **Long SP, Humphries S, Falkowski PG. 1994.** Photoinhibition of Photosynthesis in Nature.
759 *Annual Review of Plant Physiology and Plant Molecular Biology* **45**: 633-662.

760
761 **MacIntyre HL, Kana TM, Geider RJ. 2000.** The effect of water motion on short-term rates
762 of photosynthesis by marine phytoplankton. *Trends in Plant Science* **5**: 12-17.

763
764 **Mann DG, Vanormelingen P. 2013.** An inordinate fondness? The number, distributions, and
765 origins of diatom species. *Journal of Eukaryotic Microbiology* **60**: 414-420.

766
767 **Nagao R, Takahashi S, Suzuki T, Dohmae N, Nakazato K, Tomo T. 2013.** Comparison of
768 oligomeric states and polypeptide compositions of fucoxanthin chlorophyll a/c-binding
769 protein complexes among various diatom species. *Photosynthesis Research* **117**: 281-288.

770
771 **Niyogi KK, Truong TB. 2013.** Evolution of flexible non-photochemical quenching
772 mechanisms that regulate light harvesting in oxygenic photosynthesis. *Current Opinion in*
773 *Plant Biology* **16**: 307-314.

774
775 **Nymark M, Valle KC, Brembu T, Hancke K, Winge P, Andresen K, Johnsen G, Bones**
776 **AM. 2009.** An integrated analysis of molecular acclimation to high light in the marine diatom
777 *Phaeodactylum tricorutum*. *PLoS One* **4**: e7743.

778
779 **Nymark M, Valle KC, Hancke K, Winge P, Andresen K, Johnsen G, Bones AM,**
780 **Brembu T. 2013.** Molecular and photosynthetic responses to prolonged darkness and
781 subsequent acclimation to re-illumination in the diatom *Phaeodactylum tricorutum*. *PLoS*
782 *One* **8**: e58722.

783
784 **Oelze M-L, Muthuramalingam M, Vogel MO, Dietz K-J. 2014.** The link between
785 transcript regulation and de novo protein synthesis in the retrograde high light acclimation
786 response of *Arabidopsis thaliana*. *BMC genomics* **15**: 320.

787
788 **Orefice I, Chandrasekaran R, Smerilli A, Corato F, Caruso T, Casillo A, Corsaro MM,**
789 **Dal Piaz F, Ruban AV, Brunet C. 2016.** Light-induced changes in the photosynthetic
790 physiology and biochemistry in the diatom *Skeletonema marinoi*. *Algal Research* **17**: 1-13.

791
792 **Park S, Jung G, Hwang Ys, Jin E. 2010.** Dynamic response of the transcriptome of a
793 psychrophilic diatom, *Chaetoceros neogracile*, to high irradiance. *Planta* **231**: 349-360.

794
795 **Petrou K, Doblin M, Ralph P. 2011.** Heterogeneity in the photoprotective capacity of three
796 Antarctic diatoms during short-term changes in salinity and temperature. *Marine Biology* **158**:
797 1029-1041.

798

799 **Pfaffl MW, Horgan GW, Dempfle L. 2002.** Relative expression software tool (REST) for
800 group-wise comparison and statistical analysis of relative expression results in real-time PCR.
801 *Nucleic Acids Research* **30**: e36.

802

803 **Ragni M, d'Alcalà MR. 2007.** Circadian variability in the photobiology of *Phaeodactylum*
804 *tricornutum*: pigment content. *Journal of Plankton Research* **29**: 141-156.

805

806 **Roesle P, Stempfle F, Hess SK, Zimmerer J, Río Bártulos C, Lepetit B, Eckert A, Kroth**
807 **PG, Mecking S. 2014.** Synthetic polyester from algae oil. *Angewandte Chemie International*
808 *Edition* **53**: 6800-6804.

809

810 **Ruban AV, Lavaud J, Rousseau B, Guglielmi G, Horton P, Etienne AL. 2004.** The super-
811 excess energy dissipation in diatom algae: comparative analysis with higher plants.
812 *Photosynthesis Research* **82**: 165-175.

813

814 **Schaller-Laudel S, Volke D, Redlich M, Kansy M, Hoffmann R, Wilhelm C, Goss R.**
815 **2015.** The diadinoxanthin diatoxanthin cycle induces structural rearrangements of the isolated
816 FCP antenna complexes of the pennate diatom *Phaeodactylum tricornutum*. *Plant Physiology*
817 *and Biochemistry* **96**: 364-376.

818

819 **Schellenberger Costa B, Jungandreas A, Jakob T, Weisheit W, Mittag M, Wilhelm C.**
820 **2013.** Blue light is essential for high light acclimation and photoprotection in the diatom
821 *Phaeodactylum tricornutum*. *Journal of Experimental Botany* **64**: 483-493.

822

823 **Schumann A, Goss R, Jakob T, Wilhelm C. 2007.** Investigation of the quenching efficiency
824 of diatoxanthin in cells of *Phaeodactylum tricornutum* (Bacillariophyceae) with different pool
825 sizes of xanthophyll cycle pigments. *Phycologia* **46**: 113-117.

826

827 **Serôdio J, Lavaud J. 2011.** A model for describing the light response of the
828 nonphotochemical quenching of chlorophyll fluorescence. *Photosynthesis Research* **108**: 61-
829 76.

830

831 **Strzepek RF, Harrison PJ. 2004.** Photosynthetic architecture differs in coastal and oceanic
832 diatoms. *Nature* **431**: 689-692.

833

834 **Su W, Jakob T, Wilhelm C. 2012.** The impact of nonphotochemical quenching of
835 fluorescence on the photon balance in diatoms under dynamic light conditions. *Journal of*
836 *Phycology* **48**: 336-346.

837

838 **Taddei L, Stella GR, Rogato A, Bailleul B, Fortunato AE, Annunziata R, Lepetit B,**
839 **Lavaud J, Bouly J-P, Finazzi G et al. 2016.** Multi-signal control of the expression of the
840 LHCX protein family in the marine diatom *Phaeodactylum tricornutum*. *Journal of*
841 *Experimental Botany* **67**: 3939-3951.

842
843 **Tozzi S, Schofield O, Falkowski P. 2004.** Historical climate change and ocean turbulence as
844 selective agents for two key phytoplankton functional groups. *Marine Ecology Progress*
845 *Series* **274**: 123-132.

846
847 **Triantaphylidès C, Krischke M, Hoerberichts FA, Ksas B, Gresser G, Havaux M, Van**
848 **Breusegem F, Mueller MJ. 2008.** Singlet oxygen is the major reactive oxygen species
849 involved in photooxidative damage to plants. *Plant Physiology* **148**: 960-968.

850
851 **Valle KC, Nymark M, Aamot I, Hancke K, Winge P, Andresen K, Johnsen G, Brembu**
852 **T, Bones AM. 2014.** System responses to equal doses of photosynthetically usable radiation
853 of blue, green, and red light in the marine diatom *Phaeodactylum tricornutum*. *PLoS One* **9**:
854 e114211.

855
856 **van de Poll WH, Visser RJW, Buma AGJ. 2007.** Acclimation to a dynamic irradiance
857 regime changes excessive irradiance sensitivity of *Emiliana huxleyi* and *Thalassiosira*
858 *weissflogii*. *Limnology and Oceanography* **52**: 1430-1438.

859
860 **Veith T, Brauns J, Weisheit W, Mittag M, Büchel C. 2009.** Identification of a specific
861 fucoxanthin-chlorophyll protein in the light harvesting complex of photosystem I in the
862 diatom *Cyclotella meneghiniana*. *Biochimica et Biophysica Acta-Bioenergetics* **1787**: 905-
863 912.

864
865 **Wagner H, Jakob T, Lavaud J, Wilhelm C. 2016.** Photosystem II cycle activity and
866 alternative electron transport in the diatom *Phaeodactylum tricornutum* under dynamic light
867 conditions and nitrogen limitation. *Photosynthesis Research* **128**: 151-161.

868
869 **Wagner H, Jakob T, Wilhelm C. 2006.** Balancing the energy flow from captured light to
870 biomass under fluctuating light conditions. *New Phytologist* **169**: 95-108.

871
872 **Westermann M, Rhiel E. 2005.** Localisation of fucoxanthin chlorophyll a/c-binding
873 polypeptides of the centric diatom *Cyclotella cryptica* by immuno-electron microscopy.
874 *Protoplasma* **225**: 217-223.

875
876 **Wilhelm C, Büchel C, Fisahn J, Goss R, Jakob T, LaRoche J, Lavaud J, Lohr M,**
877 **Riebesell U, Stehfest K et al. 2006.** The regulation of carbon and nutrient assimilation in
878 diatoms is significantly different from green algae. *Protist* **157**: 91-124.

879
880 **Wilhelm C, Jungandreas A, Jakob T, Goss R. 2014.** Light acclimation in diatoms: From
881 phenomenology to mechanisms. *Marine genomics* **16**: 5-15.

882
883 **Wu H, Cockshutt AM, McCarthy A, Campbell DA. 2011.** Distinctive photosystem II
884 photoinactivation and protein dynamics in marine diatoms. *Plant Physiology* **156**: 2184-2195.

885
886 **Wu H, Roy S, Alami M, Green B, Campbell DA. 2012.** Photosystem II photoinactivation,
887 repair and protection in marine centric diatoms. *Plant Physiology* **160**: 464-476.

888
889 **Zaslavskaia LA, Lippmeier JC, Kroth PG, Grossman AR, Apt KE. 2000.** Transformation
890 of the diatom *Phaeodactylum tricornutum* (Bacillariophyceae) with a variety of selectable
891 marker and reporter genes. *Journal of Phycology* **36**: 379-386.

892
893 **Zhu SH, Green BR. 2010.** Photoprotection in the diatom *Thalassiosira pseudonana*: Role of
894 LI818-like proteins in response to high light stress. *Biochimica et Biophysica Acta (BBA)-*
895 *Bioenergetics* **1797**: 1449-1457.

896
897
898
899

900 **Figure legends**

901 Figure 1: Dynamic light conditions used in the experiments. One sine light (SL) and two
902 fluctuating light (FL) conditions with different intensities were applied during the daily
903 phases of the light exposure and light intensity was measured every minute.

904 Figure 2: Comparison of NPQ capacity in the four different *Phaeodactylum tricornutum*
905 strains (Pt1, Pt1sil, Pt4, Pt4ov) under SL (a) and FL (b) conditions. Time is indicated as
906 experimental day (0 to 3, separated with vertical bars/arrow) and the respective time of
907 sampling. Dynamic light conditions started on day 1 (indicated with an arrow). FL values
908 combine data from the FL 500 and FL 1000 treatment. Values represent the means \pm SE of
909 three to four different experiments.

910 Figure 3: Mean NPQ values of *Phaeodactylum tricornutum* strains Pt1, Pt1sil and Pt4 under
911 SL and FL conditions. Pt4ov was not included in the mean due to its much higher NPQ and
912 its partly unusual characteristics (cf. Fig. 2); this is exemplified by its SL 500 trace (dashed
913 line). Time is indicated as experimental day (0 to 3, separated with vertical bars/arrow) and
914 the respective time of sampling. Dynamic light conditions started on day 1 (indicated with an
915 arrow). Values represent the means \pm SE of at least six biological replicates (except Pt4ov-SL
916 500: three biological replicates).

917 Figure 4: Mean photosynthetic and photoprotective parameters of all four *Phaeodactylum*
918 *tricornutum* strains under SL and FL (500 and 1000 combined) conditions. a) Fv/Fm; b) the
919 maximum relative electron transport rate ($rETR_{max}$); c) α , the slope of the relative electron
920 transport rate versus light intensity under non-saturating light conditions; d) E_k , the
921 interception point between α and ETR_{max} , a measure for the minimal light intensity to saturate
922 photosynthesis; e) NPQ_{E_k}/NPQ_{max} , indicates the relative amount of NPQ at E_k ; f) E_{50} , the light
923 intensity, at which half of NPQ_{max} capacity is reached. Time is indicated as experimental day
924 (0 to 3, separated with vertical bars/arrow) and the respective time of sampling. Dynamic light
925 conditions started on day 1 (indicated with an arrow). Values represent the means \pm SE of at
926 least eight biological replicates. Meaning of statistical significance letters: a, values are
927 significantly different compared to day 0 ($p < 0.05$); b, values from cells exposed to FL are
928 significantly different compared to cells exposed to SL for the same time point ($p < 0.05$).

929 Figure 5: Chl a increase rate per day per culture volume (μ_{Chla}) of all four *Phaeodactylum*
930 *tricornutum* strains under SL and FL 1000 conditions. Dynamic light conditions started on
931 day 1 (indicated with an arrow). μ_{Chla} (in day^{-1}) was calculated as $\mu_{Chla} = \ln(Chl\ t_n/1.4)$, where

932 Chl t_n refers to the Chl a content measured at 18:00 during the four days of experiment (day 0
933 to day 3) and 1.4 is the Chl a content (in $\mu\text{g mL}^{-1}$) at which the cultures were adjusted to each
934 day after Chl a determination. Because data for FL 500 conditions were not complete they
935 were omitted, but, similarly to FL 1000 cells, FL 500 cells showed a higher μ_{Chla} than SL 500
936 cells. Values represent the means \pm SE of at least four biological replicates. Meaning of
937 significance letters: a, μ_{Chla} is significantly different compared to day 0 ($p < 0.05$); b, μ_{Chla} is
938 significantly different in cells exposed to FL 1000 conditions compared to cells exposed to SL
939 conditions for the same day ($p < 0.05$).

940 Figure 6: Mean diadinoxanthin and diatoxanthin (Dd+Dt) pool size (in mol (100 mol Chl a) $^{-1}$)
941 of all four *Phaeodactylum tricornutum* strains under SL and FL (500 and 1000 combined)
942 conditions. Time is indicated as experimental day (0 to 3, separated with vertical bars/arrow)
943 and the respective time of sampling. Dynamic light conditions started on day 1 (indicated with
944 an arrow). For SL conditions, data for each strain are available in Fig. S4. Values represent
945 the means \pm SE of eight biological replicates. Meaning of statistical significance letters: a,
946 Dd+Dt pool size is significantly different compared to day 0 at 17:00 ($p < 0.05$); b, Dd+Dt
947 pool size from cells exposed to the respective FL light treatment is significantly different
948 compared to cells exposed to SL for the same time point ($p < 0.05$).

949 Figure 7: Correlation of NPQ capacity versus Dd+Dt (in mol (100 mol Chl a) $^{-1}$) under SL and
950 FL (500 and 1000 combined) conditions. Values are taken from all *Phaeodactylum*
951 *tricornutum* strains except Pt4ov due to its different characteristics in NPQ (cf. Fig. 2). Time
952 is indicated as experimental day (0 to 3, separated with vertical bars/arrow) and the respective
953 time of sampling. Dynamic light conditions started on day 1 (indicated with an arrow).
954 Values represent the means \pm SE of six biological replicates. Meaning of statistical
955 significance letters: a, NPQ/(Dd+Dt) is significantly different compared to day 0 at 17:00 ($p <$
956 0.05); b, NPQ/(Dd+Dt) from cells exposed to FL is significantly different compared to cells
957 exposed to SL for the same time point ($p < 0.05$).

958 Figure 8: Relative transcript amounts of *Lhcx1* (a), *Lhcx2* (b), *Lhcx3* (c) and *Lhcf2* (d) under
959 SL and FL (500 and 1000 combined) conditions. Gene expression was normalized on
960 transcript amount of the *RPS* gene. For each gene, the expression was calculated as the mean
961 transcript amount of all *Phaeodactylum tricornutum* strains at the specific time points and
962 light conditions except for *Lhcx1* where the values of Pt4ov were omitted due to the artificial
963 *Lhcf1* promoter in this strain (c.f. Fig. S1). Dynamic light conditions started on day 1
964 (indicated with an arrow). Values represent the means \pm SE of eight biological replicates

965 (except for Lhcx1 with six biological replicates), and each biological replicate was measured
966 in technical triplicates. Meaning of significance letters: a, Gene is significantly differentially
967 expressed compared to day 0 ($p < 0.05$); b, Gene from cells exposed to FL is significantly
968 differentially expressed compared to cells at the corresponding time point exposed to SL ($p <$
969 0.05).

970 Figure 9: Mean of relative protein expression of Lhcx1 (a), Lhcx2 (b) and Lhcx3 (c) of all
971 *Phaeodactylum tricornutum* strains under SL and FL 1000 conditions, respectively. For
972 Lhcx1, protein expression data of Pt4ov were omitted due to the artificial regulation by the
973 *Lhcf1* promoter (c.f. Fig. S1). Dynamic light conditions started on day 1 (indicated with an
974 arrow). Values represent the means \pm SE of at least four biological replicates (except for
975 Lhcx1 with at least three biological replicates). Meaning of significance letters: a, protein is
976 significantly differentially expressed compared to day 0 ($p < 0.05$); b, protein from cells
977 exposed to FL is significantly differentially expressed compared to cells at the corresponding
978 time point exposed to SL ($p < 0.05$).

979 Figure 10: Correlation of relative Lhcx2 protein content *versus* NPQ increase under SL
980 conditions. NPQ was calculated as $NPQ_{\text{day}1,2,3} - NPQ_{\text{day}0}$, always measured at the 14:00 time
981 point. The three data points correspond to the Lhcx2 protein amount *versus* NPQ on day 1,
982 day 2 and day 3. Values for NPQ and Lhcx2 protein content are the means \pm SE of all
983 *Phaeodactylum tricornutum* strains except Pt4ov.

984

985

986 Supporting information (SI) can be found in a separate sheet. It contains:

987

988 Table S1: Photophysiological parameters used in this study

989

990 Fig. S1: Transcript levels of *Lhcx1* - *Lhcx3* and *Lhcf2* genes under SL and FL conditions in all
991 four *P. tricornutum* strains

992

993 Fig. S2: Fx/Chl a and Chl c/Chl a content of all four *P. tricornutum* strains under SL and FL
994 conditions

995

996 Fig. S3: Dd+Dt pool size in the four individual *P. tricornutum* strains during SL and FL
997 conditions

998

999 Fig. S4: De-epoxidation state of all four *P. tricornutum* strains under SL and FL conditions

1000

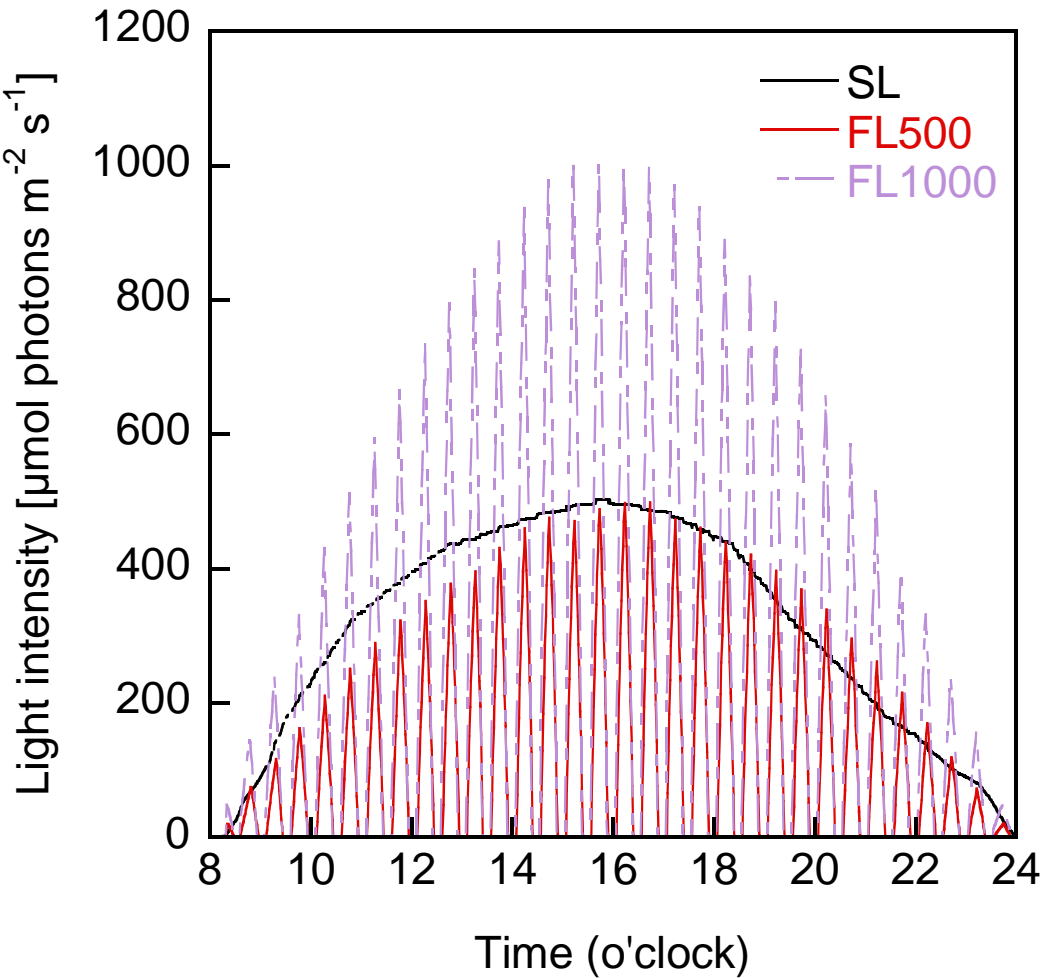
1001 Fig. S5: Lhcx protein expression in Pt4 during SL and FL conditions

1002

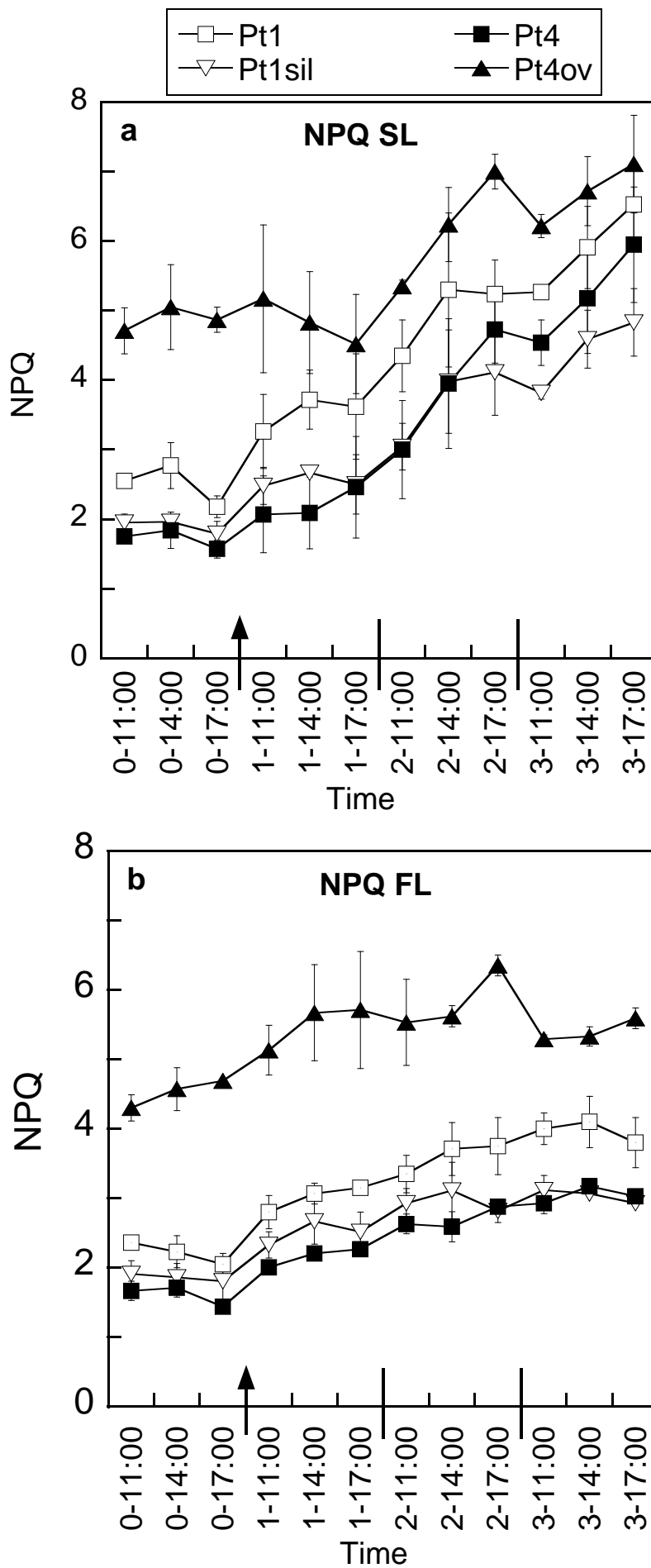
1003

Figures

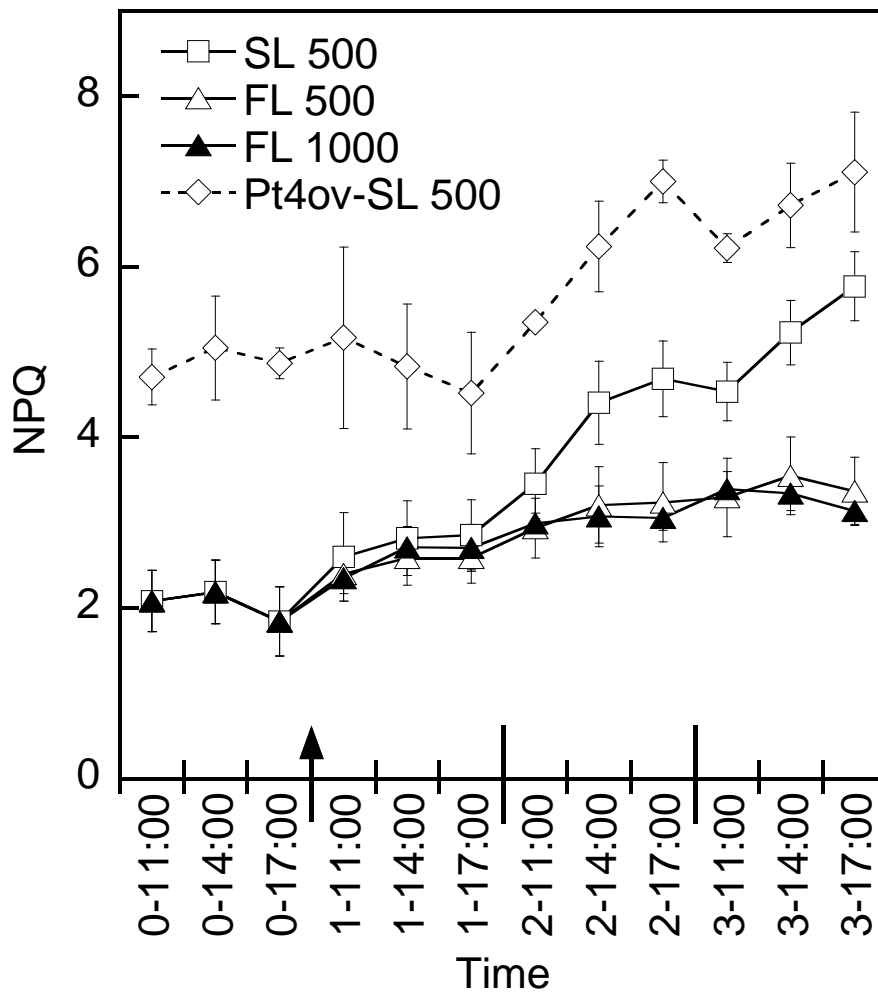
Lepetit et al., Fig. 1

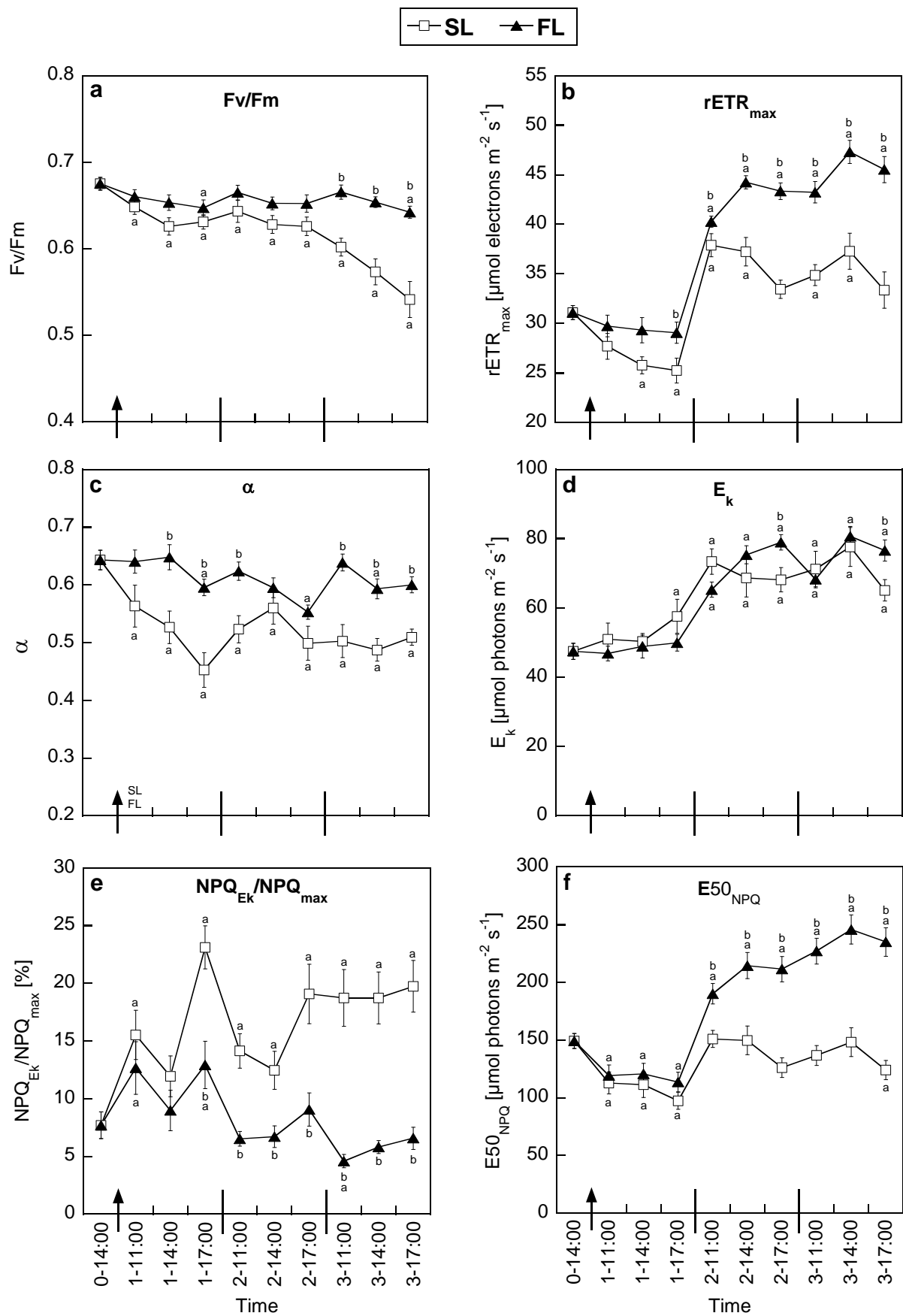


Lepetit et al., Fig. 2

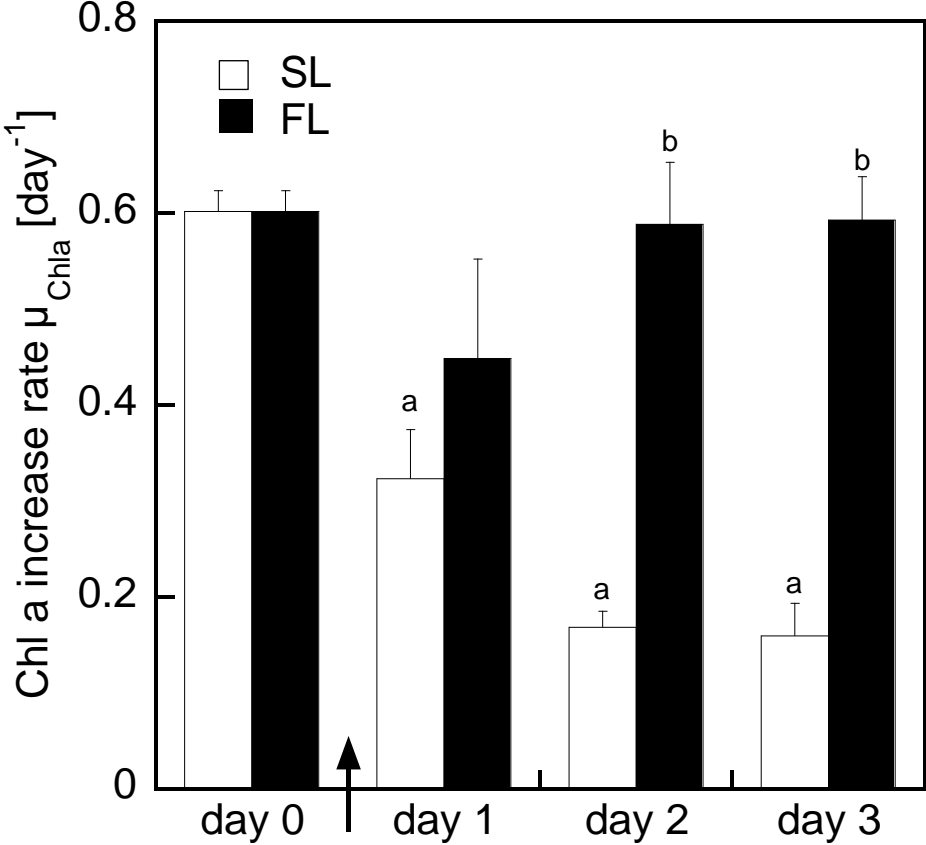


Lepetit et al., Fig. 3

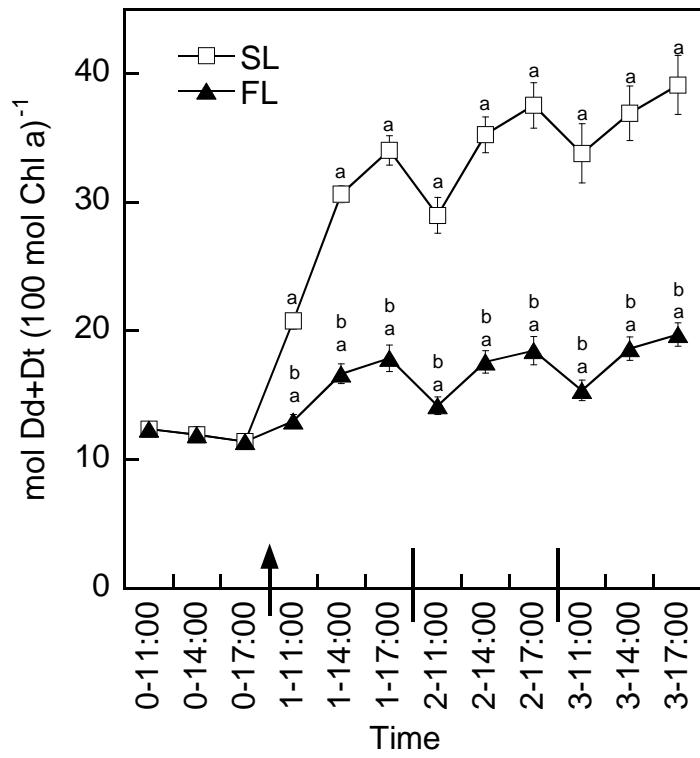




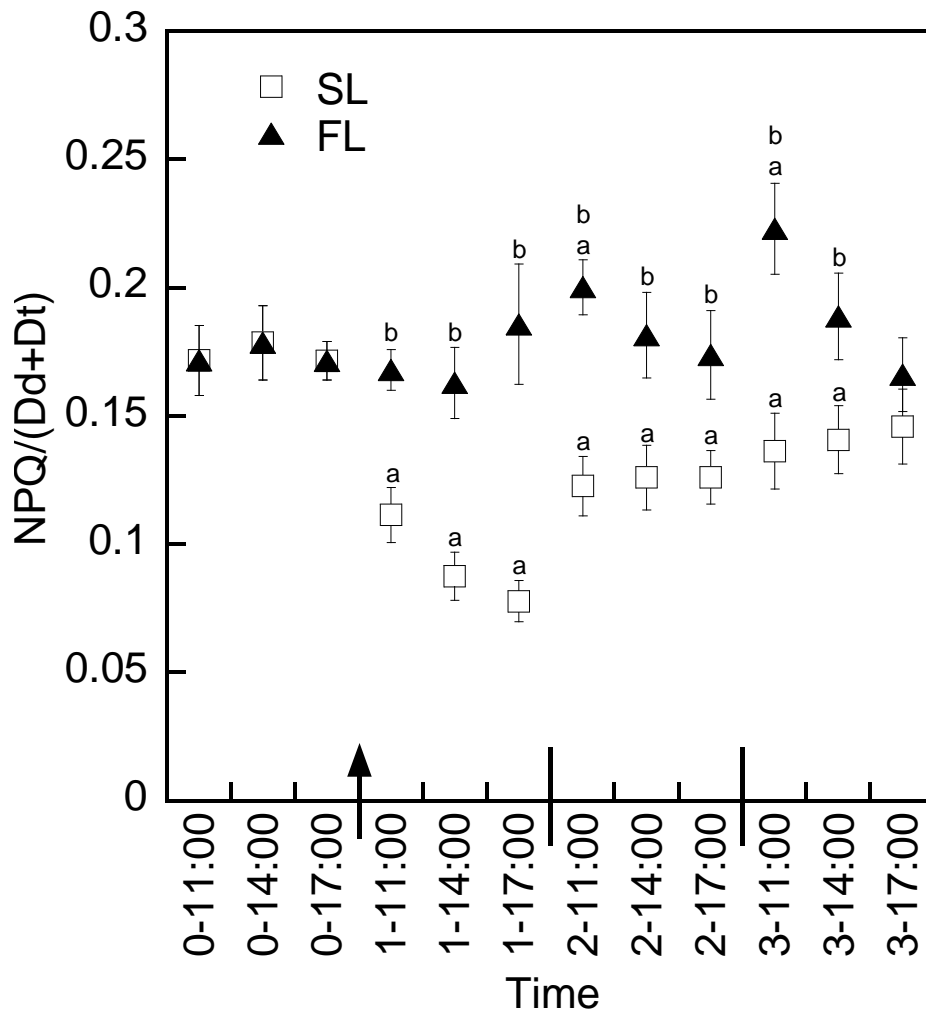
Lepetit et al., Fig. 5



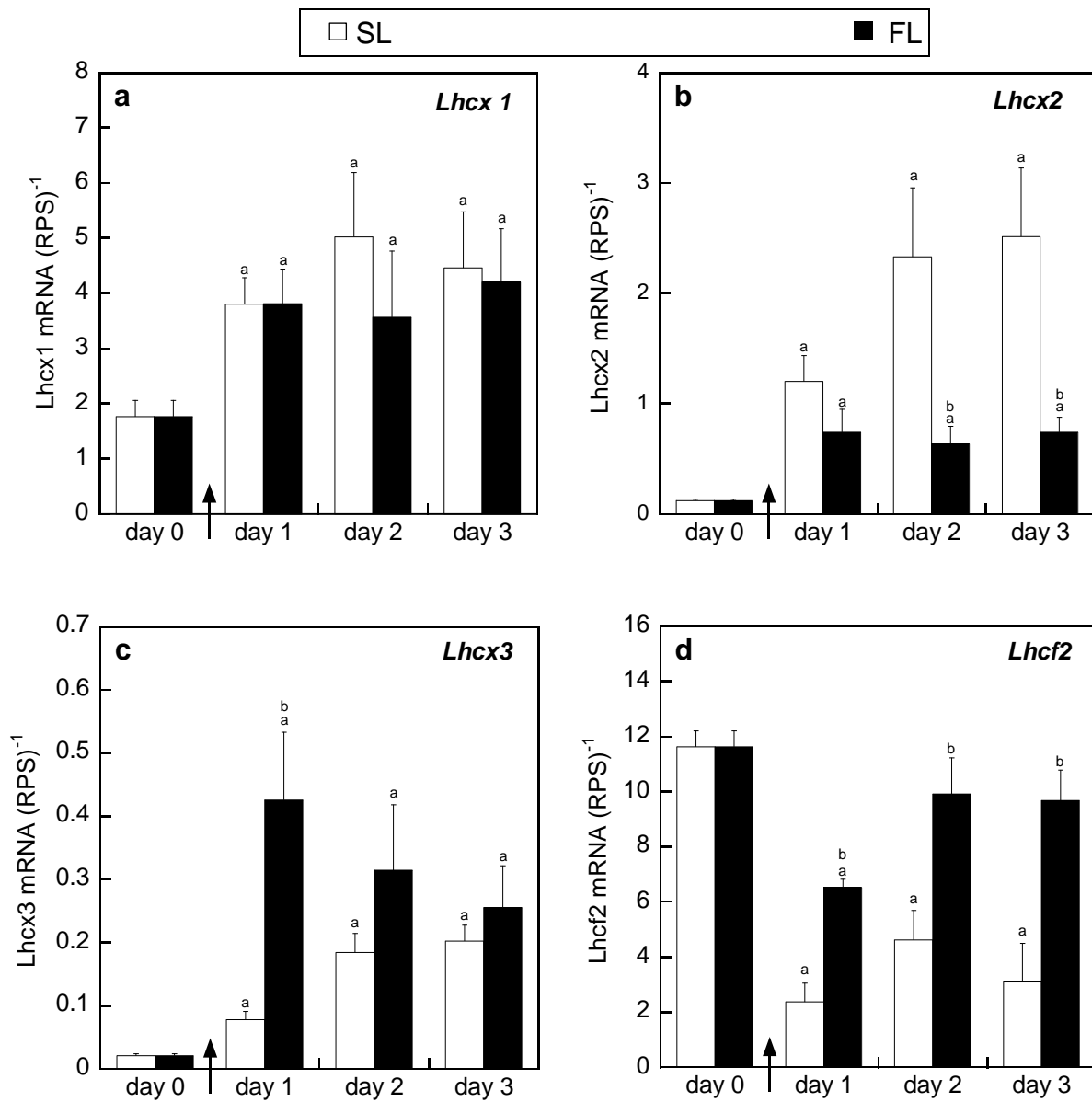
Lepetit et al., Fig. 6



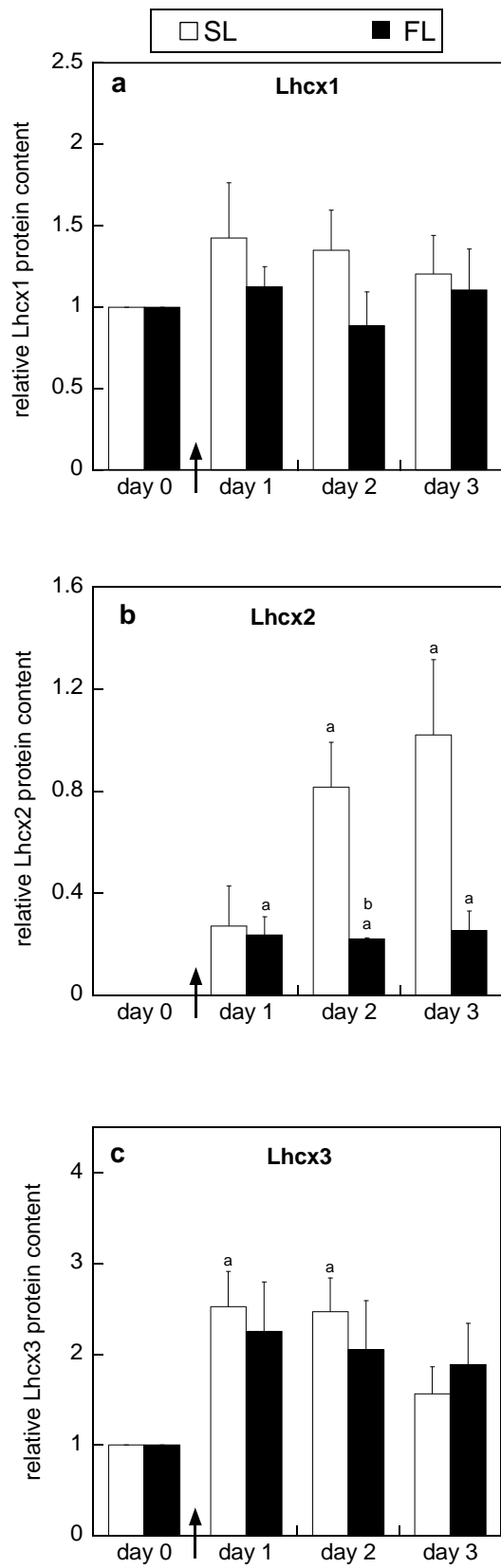
Lepetit et al., Fig. 7



Lepetit et al., Fig. 8



Lepetit et al., Fig. 9



Lepetit et al., Fig. 10

